CrystEngComm

Accepted Manuscript

This is an *Accepted Manuscript*, which has been through the Royal Society of Chemistry peer review process and has been accepted for publication.

Accepted Manuscripts are published online shortly after acceptance, before technical editing, formatting and proof reading. Using this free service, authors can make their results available to the community, in citable form, before we publish the edited article. We will replace this *Accepted Manuscript* with the edited and formatted *Advance Article* as soon as it is available.

You can find more information about *Accepted Manuscripts* in the Information for Authors.

Please note that technical editing may introduce minor changes to the text and/or graphics, which may alter content. The journal's standard Terms & Conditions and the Ethical guidelines still apply. In no event shall the Royal Society of Chemistry be held responsible for any errors or omissions in this *Accepted Manuscript* or any consequences arising from the use of any information it contains.

ROYAL SOCIETY OF CHEMISTRY

www.rsc.org/crystengcomm

Please do not adjust margins

CrystEngComm

HIGHLIGHT

Porphyrinic metal-organic frameworks from custom-designed porphyrins

Received 00th January 20xx,
Accepted 00th January 20xx

DOI: 10.1039/x0xx00000x

www.rsc.org/

Seong Huh,[a] Sung-Jin Kim[b] and Youngmee Kim*[b]

This paper highlights porphyrinic metal-organic frameworks (porph-MOFs) assembled from metal ions and custom-designed porphyrins. The contents are divided into three sections based on the types of polytopic porphyrin bridging ligands in porph-MOFs: (1) porph-MOFs containing 5,10,15,20-tetra(4-pyridyl)porphyrinato (TPyP) ligand and other pyridyl-based porphyrin bridging ligands, (2) porph-MOFs containing 5,10,15,20-tetrakis(4-carboxyphenyl)porphyrinato (TCPP) ligand and other carboxyphenyl-based porphyrin bridging ligands, and (3) porph-MOFs containing other custom-designed porphyrin-based bridging ligands.

Introduction

Metal-organic frameworks (MOFs) and porous coordination polymers (PCPs) are crystalline inorganic-organic hybrid materials assembled from a metal ion or metal cluster as a node and a polytopic organic bridging ligand as a strut linker.[1] Several MOFs and PCPs are considered to be zeolite-like porous materials because of their close similarities with crystalline zeolite framework structures.[2] Zeolites containing atomic crystalline framework structures are of significant importance in a wide range of industrial applications, such as ion exchangers, sorbent materials, and catalysts for the petrochemical industry.[3] Despite the high hydrothermal stability of porous zeolites relative to MOFs, MOFs are often more attractive alternatives due to their diverse pore structures and functionalities with which zeolites cannot compete.

Porphine is a biologically important fully conjugated 18π-electron-containing macrocyclic compound shown in Scheme 1a.[4] Porphines with substituents are called porphyrins. The chemical structure of the representative porphyrin molecule, 5,10,15,20-tetraphenylporphyrin (H_2TPP) or *meso*-tetraphenylporphyrin, is depicted in Scheme 1b. Metallated porphyrin or metalloporphyrin, such as Fe-porphyrin, is an important co-factor of oxygen-transporting hemoglobin in vertebrates.[5] In addition to biological importance, a plethora

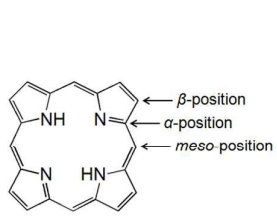

Scheme 1 The chemical structures of porphine (a) and 5,10,15,20-tetraphenylporphyrin (b).

of porphyrin molecules containing peripheral substituents at the *meso*- and *β*-positions are frequently employed in the chemical world for a wide range of sophisticated applications.[6]

In addition, porphyrin molecules can act as attractive bridging ligands in building MOFs because of their rigid molecular structure, tunable peripheral substituents in a controlled manner, large physical dimensions, and additional metallation site in the core. In turn, porphyrinic MOFs (porph-MOFs) can be utilized for a variety of applications, including gas sorption, selective catalysis, photosensitization, and photovoltaics. In particular, metalloporphyrin-based linkers can be interconnected by metal ions or metal carboxylate clusters to form porph-MOFs, which have received much attention in the last two decades, and many excellent reviews for reported porph-MOFs have been addressed by Goldberg, Choe, Wu, and Ma.[7-11]

Square planar building blocks based on tetraarylporphyrin, such as 5,10,15,20-tetra(4-pyridyl)porphyrin (H_2TPyP)[8] and 5,10,15,20-tetrakis(4-carboxyphenyl)porphyrin (H_6TCPP),[9,11] have been used extensively as metalloligands in the synthesis of porph-MOFs. They can offer two distinct metal binding

[a] *Department of Chemistry and Protein Research Center for Bio-Industry, Hankuk University of Foreign Studies, Yongin 17035, Republic of Korea.*
[b] *Department of Chemistry and Nano science, Ewha Womans University, Seoul 03760, Republic of Korea. E-mail: ymeekim@ewha.ac.kr; Fax: +82-2-3277-3419; Tel: +82-2-3277-4164*

† Footnotes relating to the title and/or authors should appear here.
Electronic Supplementary Information (ESI) available: [details of any supplementary information available should be included here]. See DOI: 10.1039/x0xx00000x

CrystEngComm Accepted Manuscript

Please do not adjust margins

sites: a functional metal binding site within the porphyrin core and a metal binding site at the carboxy and pyridyl ligands.

Because many reviews of porph-MOFs assembled from TPyP or TCPP have been reported,[7-11] this Highlight mainly focuses on the recent functional porph-MOFs containing various derivatives of TPyP and TCPP ligands, so-called custom-designed porphyrins, allowing specific applications. In addition, we summarize all of the porph-MOFs containing porphyrin-based bridging ligands in chronological order since the first ZnTPyP was used as a building block for a chain-oligomeric one-dimensional (1D) polymer (Table 1 and Table 2).[12]

This Highlight is divided into three sections: (1) porph-MOFs containing TPyP and other pyridyl-based ligands, (2) porph-MOFs containing TCPP and other carboxyphenyl-based ligands, and (3) porph-MOFs containing other custom-designed porphyrin-based bridging ligands.

Pyridyl-based porphyrinic MOFs (or porph-MOFs containing TPyP and derivatives)

Pyridyl-based porphyrin ligands used in the construction of porphyrinic frameworks are listed in Scheme 2, and Table 1 summarizes the porphyrinic coordination polymers (porph-CPs) and porph-MOFs containing pyridyl-based porphyrins.[12-59] Some research groups have reported reviews on CPs and MOFs containing pyridyl-based porphyrins.[7,8]

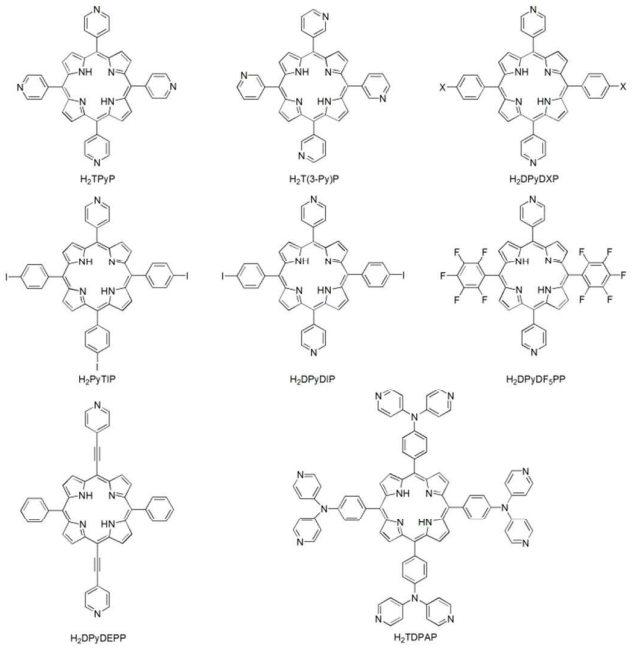

Scheme 2 Pyridyl-based porphyrin ligands for porph-MOFs: H_2TPyP = 5,10,15,20-tetra(4-pyridyl)porphyrin, H_2T(3-Py)P = 5,10,15,20-tetra(3-pyridyl)porphyrin, H_2DPyDXP (X = H, CN, Cl, CH_3, OH, or CF_3) = 5,10-dipyridyl-10,20-diarylporphyrin, H_2PyTIP = 5-(4′-pyridyl)-10,15,20-tris(4′-iodophenyl)porphyrin, H_2DPyDIP = 5,15-bis(4′-pyridyl)-10,20-bis(4′-iodophenyl)porphyrin, H_2DPyDF$_5$PP = 5,15-dipyridyl-10,20-bis(pentafluorophenyl))porphyrin, H_2TDPAP = 5,10,15,20-tetrakis(4,4′-dipyridylaminophenylene)porphyrin.

Tetrapyridylporphyrin: H_2TPyP (5,10,15,20-tetra(4-pyridyl)porphyrin)

H_2TPyP has been widely used for the construction of porph-MOFs. Over the past two decades, numerous porph-CPs and porph-MOFs containing pyridyl-based porphyrins have been reported. The porph-CPs and porph-MOFs containing either free-base H_2TPyP or metallated MTPyP as building blocks can be classified into 1D, 2D, and 3D structures.

The CPs containing free-base H_2TPyP as a building block provide mostly 1D or 2D structures[15,18-20,23,24,26,38] and 3D frameworks[32,46] with the aid of the connecting Cd^{II} ion, and hybrid assemblies of H_2TPyP and aqua nitrates of lanthanoid ions produce 3D networks through hydrogen bonds.[38,39]

Self-assembly of MTPyP units (M = Zn^{II}, Fe^{II}, Co^{II}, or Mn^{II}) has led to ladder-type 1D structures;[21] a 1D ribbon type for Zn^{II};[29] a 2D paddlewheel-like pattern for Fe^{II};[22] a 2D square grid network for Zn^{II};[40] and 3D hexagonal networks for Co^{II}, Mn^{II},[16] and Zn^{II}.[27,28,56]

Networks self-assembled from MTPyP units and external metal ions included axial coordination to the metals on the porphyrin cores to form 3D frameworks.[13,14,17,24,32,47,49] MTPyP units also can be interconnected by the metal ions or secondary building unit (SBU) to form a 2D square grid network.[31,32,37,41,42] Choe and coworkers classified the structural motifs of porph-CPs assembled from H_2TPyP and its derivatives in 2009.[8]

Wu and coworkers reported a 3D porous porph-MOF in which a tetradentate metalloligand Sn^{IV}TPyP bridges four Zn^{II} ions to form a 2D framework structure lying in the crystallographic *ab*-plane, and two porphyrin units are further coupled together by a formate strut to coordinate two Sn atoms to extend into a 3D porous network (Fig. 1).[47] This 3D porous MOF showed remarkably high photocatalytic activities for the oxygenation of phenol and sulfides, resulting in excellent yields and remarkable selectivity in heterogeneous phases.

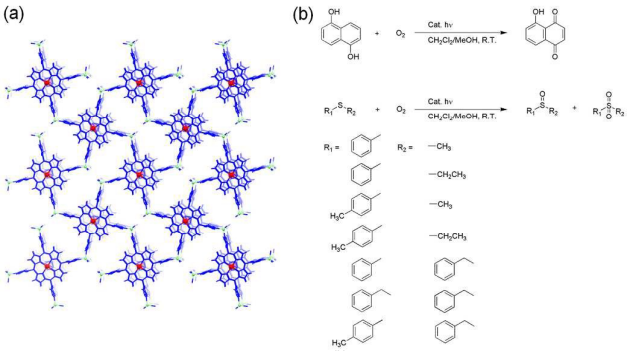

Fig. 1 (a) 3D network of $[Zn_2(H_2O)_4Sn^{IV}(TPyP)(HCOO)_2]$. (b) Photocatalytic oxygenation reaction.

Li, Wu, and coworkers synthesized a layered hybrid material of polyoxometalate–Mn^{III}–metalloporphyrin.[49] They used a new two-step synthetic method to overcome the low miscibility problem of reactants – water soluble polyoxoanions and organic solvent soluble porphyrins. The zwitterionic complex, $\{[Mn^{III}(DMF)_2TPyP](PW_{12}O_{40})\}^{2-}$ (DMF = *N*,*N*-dimethylformamide), was first formed, and subsequently the reaction of mixture of the zwitterionic complex and

CrystEngComm Accepted Manuscript

This journal is © The Royal Society of Chemistry 20xx

$Cd(NO_3)_2{\cdot}4H_2O$ in DMF and acetic acid at 80 ℃ for 48 h was successfully carried out to form a layered hybrid material. The hybrid material exhibited a remarkable capability for scavenging dyes and for selective heterogeneous oxidation of alkylbenzenes with excellent product yields and 100% selectivity (Fig. 2).[49]

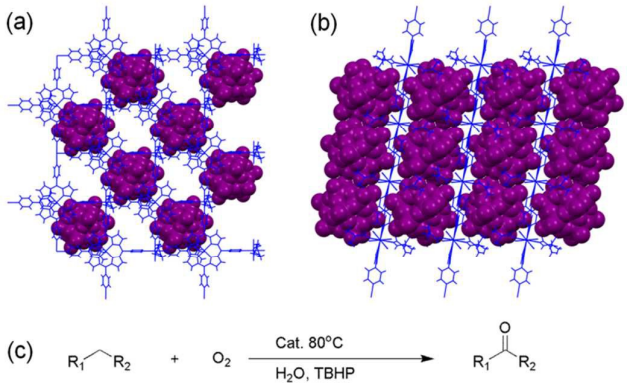

Fig. 2 (a) 2D network of $[Cd(DMF)_2Mn^{III}(DMF)_2TPyP]_n^{3n+}$ and a layer of the $[PW_{12}O_{40}]^{3-}$ polyoxoanions along the *c*-axis. (b) Packing diagram along the *b*-axis. (c) Catalytic oxidation reaction of alkylbenzenes.

Chao and coworkers reported a novel thermoresponsive solid framework, HMOF-1 (hinged metal-organic framework-1), assembled from H_2TPyP and CdI_2 and exhibiting a 3D "lattice fence" topology with extraordinary thermal expansion and shrinkage behaviours (Fig. 3).[46]

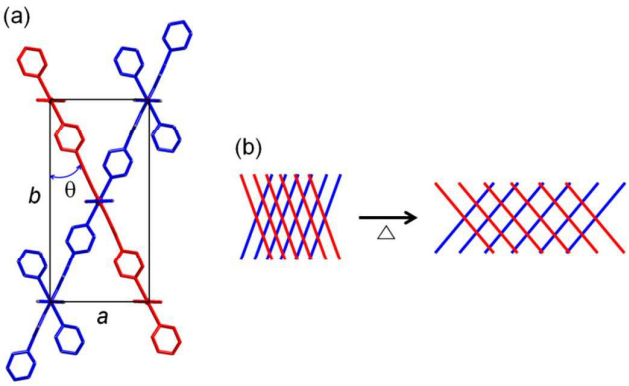

Fig. 3 (a) The simplified crystal structure of HMOF-1 along the *c*-axis showing the hinge angle θ. (b) Illustration of the "lattice fence" showing hinged expansion upon heating.

Mukherjee and coworkers reported the self-assembly of a nanoscopic $Pt_{12}Fe_{12}$ heterometallic open hexagonal box containing six faces occupied by H_2TPyP linkers (Fig. 4).[33] The nano-sized porphyrin molecular box displayed enhanced solution fluorescence upon binding of Zn^{II} ions.

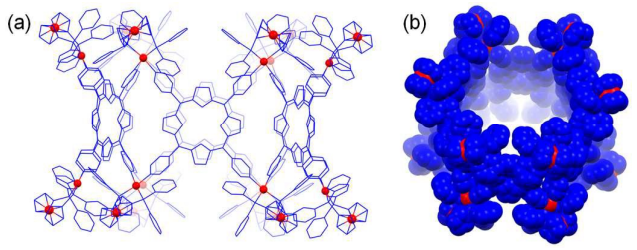

Fig. 4 (a) Molecular structure of the hexagonal porphyrin box. (b) The CPK view of the hexagonal porphyrin box. Large accessible windows are discernible.

A novel catalytic system based on the immobilization of a Mn^{III} tetrapyridylporphyrin catalyst (Mn(TPyP)OAc) on magnetic core-shell nanoparticles (silica-coated magnetite nanoparticles, Fe_3O_4-SiO_2) has been developed (Fig. 5).[54] This immobilized catalyst showed excellent catalytic capability in the oxidation of alkenes and alkanes and could be reused at least six times without loss of its activity.

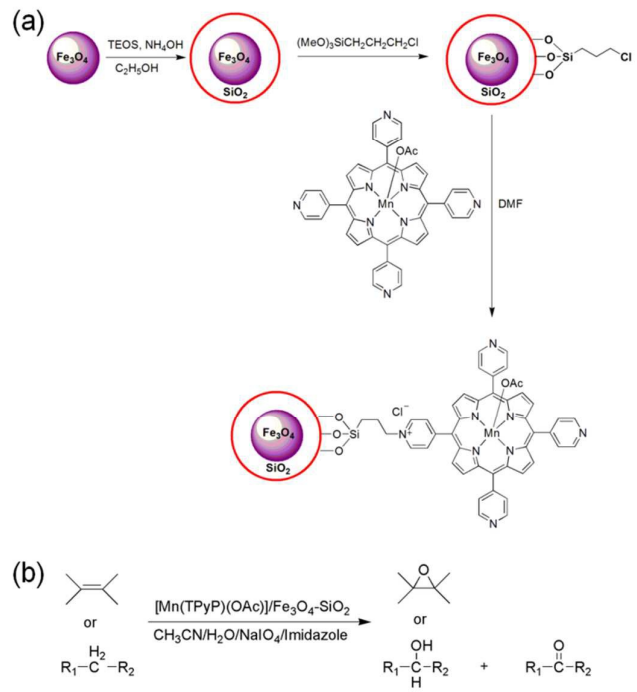

Fig. 5 (a) Preparation of the magnetically separable porphyrin-based core-shell catalyst. (b) Epoxidation of alkenes and hydroxylation of alkanes with $NaIO_4$ catalyzed by [Mn(TPyP)OAc]/Fe_3O_4-SiO_2.

Huang and coworkers tuned the size of CuTPyP dispersed nanoplates, assembled nanoplates, and microspindles fabricated by a simple surfactant-assisted solution route.[48] Liu, Lin, and coworkers reported multi-strand metallo-supramolecular polymers self-assembled by pyridyl-functionalized porphyrin derivatives on a Au(111) surface through pyridyl–Cu–pyridyl coordination.[50] Makiura and coworkers generated smooth ultrathin MOF nanosheets, NAFS-21, and the NAFS-21 nanosheets were assembled by the interfacial reaction between tetratopic CuTPyP and structure-directing Cu^{II} ion joints.[55]

CrystEngComm Accepted Manuscript

Tetrapyridylporphyrin: $H_2T(3\text{-Py})P$ (5,10,15,20-tetra(3-pyridyl)porphyrin)

Porph-CPs and porph-MOFs containing free-base $H_2T(3\text{-Py})P$ and metallated MT(3-Py)P were reported by Boyd,[30] Choe,[43] and Goldberg[39,44,45] ($H_2T(3\text{-Py})P$ = 5,10,15,20-tetra(3-pyridyl)porphyrin). $H_2T(3\text{-Py})P$ is the porphyrin building block in which the N atoms in the pyridyl ring are in different positions from those of H_2TPyP. The structure of the building block, $H_2T(3\text{-Py})P$, is shown in Scheme 1. $H_2T(3\text{-Py})P$ has been used in the construction of porphyrinic supramolecular assemblies through either coordination or hydrogen bonding interactions.[45]

A flexible, interdigitated, 2D porphyrin framework MPF-3 (MPF = metalloporphyrin framework) was synthesized by the solvothermal reaction of $H_2T(3\text{-Py})P$ and $Zn(NO_3)_2{\cdot}6H_2O$ in DMF.[43] The Zn^{II} centre on the porphyrin core is axially connected to the neighbouring pyridyl of ZnT(3-Py)P to form a 2D porphyrinic layer in which two out of four available pyridyl groups were used for the construction of the 2D layer (Fig. 6). The uncoordinated pyridyl groups provided interdigitated 2D layers. The topology of the MPF-3 structure is closely related to Cairo pentagonal tessellation. The MPF-3 framework was exposed to several different guest molecules, and X-ray powder diffraction data indicated that the movement of the 2D layers depends on the choice of guest molecule.

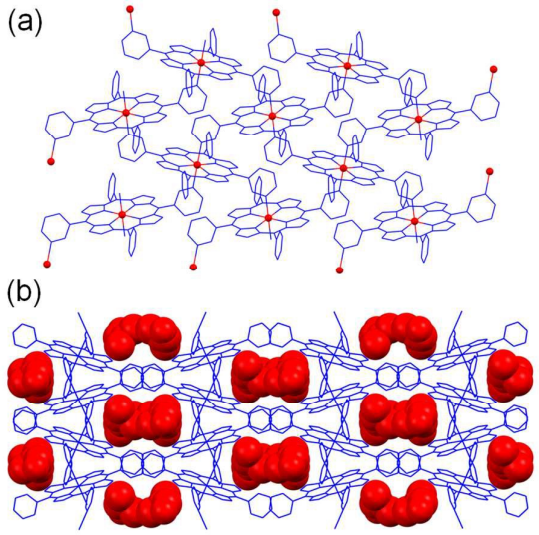

Fig. 6 (a) 2D layer of MPF-3 along the *a*-axis. (b) Interdigitated layers with 1D solvent channels. The red CPK indicates DMF molecules.

Study of the supramolecular reactivity of $H_2T(3\text{-Py})P$ building blocks in the context of crystal engineering was explored by Goldberg and coworkers.[44] Reactions of $H_2T(3\text{-Py})P$ with $CuCl_2$ and $MnCl_2$ afforded hybrid CPs with uniquely interesting and novel architectures of 3D connectivity, in which the metal ions have multiple oxidation states (Fig. 7a and 7b). Crystalline adducts from $H_2T(3\text{-Py})P$ and aqua nitrate salts of lanthanoid metal ions showed several different intermolecular associations (Fig. 7c). From the results, the $H_2T(3\text{-Py})P$ building blocks can effectively be employed for supramolecular construction with transition metal ions, either through direct coordination to the metal centre or by hydrogen bonding to their coordination sphere ligands, as well as in multiporphyrin self-hydrogen-bonded networks.

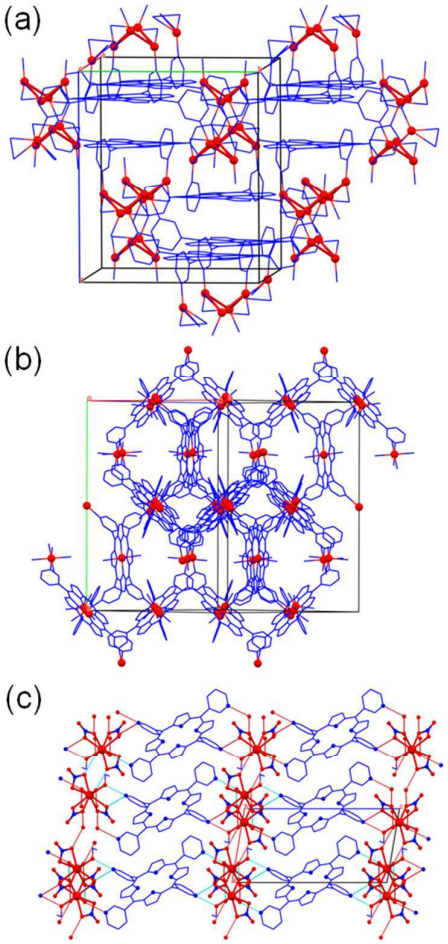

Fig. 7 (a) 3D polymeric structure of $Cu^{II}T(3\text{-Py})P$ tessellated by tetranuclear $(Cu^{I}Cl)_4$. (b) 3D polymer of a mixture of $Mn^{II}T(3\text{-Py})P$ and $Mn^{IV}Cl_2T(3\text{-Py})P$ entities, tessellated by $Mn^{II}Cl_2$ and $Mn^{III}Cl_3$ connectors. (c) Crystal structure of $H_2T(3\text{-Py})P{\cdot}2[Yb^{III}(NO_3)_3(H_2O)_2(EtOH)]{\cdot}o\text{-DCB}$ (*o*-DCB = *o*-dichlorobenzene), showing the hydrogen bonding (green lines) between the interacting components.

The 2D self-coordinated polymer of $Co^{II}T(3\text{-Py})P$, $[Co^{II}T(3\text{-Py})P]{\cdot}2DMF$ with the DMF molecules between the 2D layers, 3D polymers of either free-base $H_2T(3\text{-Py})P$ or metallated Cd(DMF)T(3-Py)P interlinked by $CdCl_2$ exocyclic inter-porphyrin connectors, and a 3D polymer of $Cu^{II}T(3\text{-Py})P$ tessellated by tetranuclear $(Cu^{I}Br)_4$ linkers were also synthesized by Goldberg (Fig. 8).[45]

H_2TPyP and $H_2T(3\text{-Py})P$ linkers were also used for the supramolecular assembly of fullerene (C_{60}) and porphyrin motifs.[23,30] $Pb(NO_3)_2$, $HgBr_2$, and HgI_2 connect H_2TPyP and $H_2T(3\text{-PyP})$ to form sheets, and fullerenes are intercalated between sheets of $M(H_2TPyP)$ or $M[H_2T(3\text{-Py})P]$. These assemblies are connected by close $C_{60}{\cdots}$porphyrin $\pi{\cdots}\pi$ interactions, leading to the alignment of the porphyrins into linear alternating fullerene porphyrin columns.[30]

CrystEngComm Accepted Manuscript

This journal is © The Royal Society of Chemistry 20xx

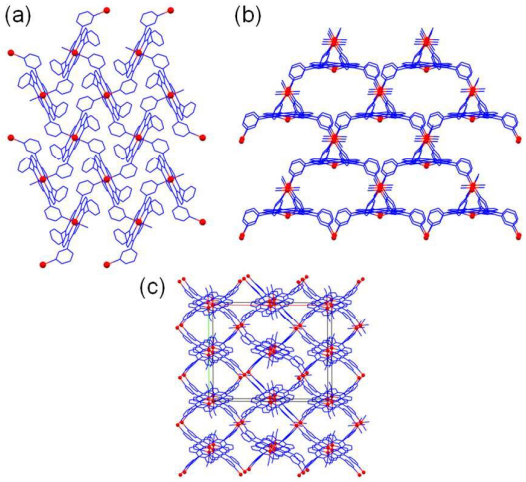

Fig. 8 (a) 2D network of CoT(3-Py)P. (b) 3D coordination network between the CdT(3-Py)P and the $CdCl_2$ constituents. (c) A single-framework polymeric architecture sustained by the $CdCl_2$ connectors.

Dipyridylporphyrin: H_2DPyDXPP (5,10-Dipyridyl-10,20-diarylporphyrin, X = H, CN, OCH_3, OH, CF_3, Cl, or I)

Porphyrin derivatives based on two 4-pyridyl groups at the 5- and 15-*meso*-positions and two 4-aryl moieties bearing various groups (H,[57] CH_3,[58] I,[34] CN,[35,59] Cl,[59] OCH_3,[35] OH[35] and CF_3[35]) at the 10- and 20-*meso*-positions were used for the construction of porph-CPs or porph-MOFs (Scheme 2).

H_2DPyDXPP (5,10-dipyridyl-10,20-diarylporphyrin, X = CN, OCH_3, or OH) with Zn^{II} ions constructed robust 3D frameworks with hexagonal channels through slow diffusion of $CHCl_3$ solutions of H_2DPyDXPP ligands into a CH_3OH solution of $Zn(OAc)_2{\cdot}2H_2O$.[35] They showed large void volumes (calculated by Platon software, solvent molecules virtually removed) of 277 Å^3, 250 Å^3, and 463 Å^3, respectively. These voids can be compared with the isostructural network from TPyP (585 Å^3).[27] H_2DPyDCF$_3$PP bearing two CF_3 groups with a Zn^{II} cation provided either 3D or 1D networks.[35] H_2DPyDIPP (5,15-bis(4′-pyridyl)-10,20-bis(4′-iodophenyl)porphyrin) also constructed a robust solid framework with extended honeycomb architecture by polymeric self-coordination in the presence of a Zn^{II} ion[34] with a void volume of 302 Å^3. From the comparison of voids, both the size and polarity of the pores were tuned by the nature of the substituents attached to the two aryl groups.[35] H_2PyTIPP (5-(4′-pyridyl)-10,15,20-tris(4′-iodophenyl)porphyrin) and H_2DPyDIPP moieties formed extended supramolecular layers held together by intermolecular N···I and I···π interactions and π···π stacking in an offset manner to yield layered crystals. The metallated monopyridyl derivative Co-PyTIPP assembled into a cyclic tetrameric structure.[34]

Co-MOF, $[Co(DpyDtolP)]_6{\cdot}12H_2O$, composed of DpyDtolP (also called $DPyDCH_3PP$, 5,15-di(4-pyridyl)-10,20-di(4-methylphenyl)porphyrin) was prepared by thermal reaction in DMF at 120 ℃ for 48 h in high yield,[58] and its structure is an exceptionally highly stable 3D network that is isostructural with $[ZnTPyP]_6$.[27] The crystal structure of CO_2-captured Co-MOF revealed that the linear arrangement of the CO_2 molecules occupied the micropores, and iodine-captured Co-MOF revealed a linear arrangement of polyiodine chains in the micropores exhibiting electrically conducting behaviour. Additionally, the separately prepared microscale sample, micro-Co-MOF, exhibited an enhanced uptake of iodine compared to the bulk Co-MOF under the same conditions (Fig. 9).[58] Additionally, two isostructural porous Co-MOFs, $[Co(DpyDClP)]_6{\cdot}18H_2O$ and $[Co(DpyDCNP)]_6{\cdot}18H_2O$ (DpyDClP = 5,15-di(4-pyridyl)-10,20-di(4-chlorophenyl) porphyrin; DpyDCNP = 5,15-di(4-pyridyl)-10,20-di(4-cyanophenyl)porphyrin), were reported by Huh, Lee, Kim and coworkers.[59] Despite the same framework structures, $[Co(DpyDClP)]_6$ exhibited a higher uptake of CO_2 at 196 K than $[Co(DpyDCNP)]_6$ due to its larger void volume.

Simple dipyridylporphyrin, H_2DPyP (5,10-dipyridyl-10,20-diphenylporphyrin) based on two 4-pyridyl groups at the 5- and 15-*meso*-positions and two simple 4-phenyl groups at the 10- and 20-*meso*-positions provided 1D double-chain PCPs with Co^{II} or Zn^{II} ions (Fig. 10).[57] Each 1D double chain interacted with another 1D double chain by multiple hydrogen bonding to stabilize the resulting framework, resulting in solvent-free 1D double-chain PCPs with permanent porosity and highly selective adsorption of CO_2 over N_2, H_2, and CH_4 at low temperatures.

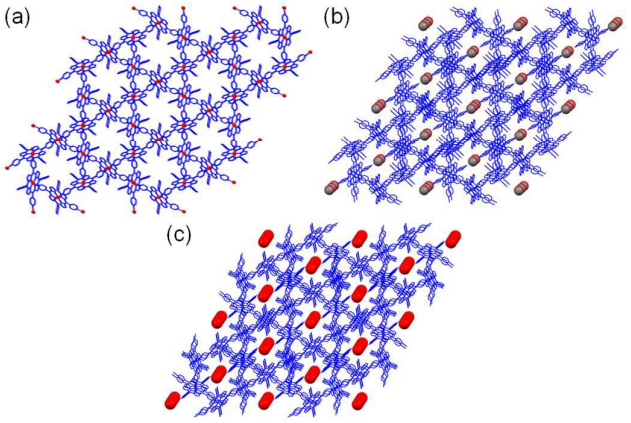

Fig. 9 (a) 3D structure of a solvent-free Co-MOF indicating hexagonally arranged micropores. (b) The linear arrangement of the CO_2 molecules occupied the inside of the micropores of Co-MOF. (c) Iodine-captured Co-MOF revealing a linear arrangement of polyiodine chains in the micropores.

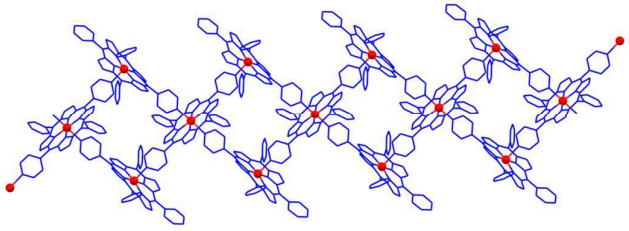

Fig. 10 1D double chain structure of $Co_3(DPyP)_3$.

H_2TDPAP (5,10,15,20-tetrakis(4,4′-dipyridylaminophenylene)-porphyrin)

CrystEngComm Accepted Manuscript

The syntheses of new porphyrin-based ligands are very attractive for the construction of porph-CPs or porph-MOFs with novel structures and intriguing properties. For example, H_2TDPAP provided various framework structures with different metal ions (Mn^{II}, Cu^{II}, Zn^{II}, or Cd^{II}) in different coordination modes, and four types of coordination modes were reported by Xie (Scheme 3).[51] $[Cl_2(H_2O)_2]^{2-}$ moieties were interconnected by free-base H_2TDPAP linkers to form a 1D structure by the solvothermal reaction in H_2O/CH_3OH at 120 ℃ (a). The metallated porphyrins, Mn^{II}TDPAP were connected by Mn^{III} ions to form interpenetrated 2D coordination networks that were further linked by $\pi\cdots\pi$ stacking interactions to afford a 3D structure by the solvothermal reaction in CH_3CN/DMF at 120 ℃ for 90 h (b), and Cu^{II}TDPAP linkers were connected by Cu^{II} ions to form a 2D sheet composed of 50- and 70-membered metallomacrocycles by the solvothermal reaction in DMF/HOAc/H_2O at 150 ℃ for 90 h (c). H_2TDPAP with Zn^{II} ions provided 1D zigzag coordination chains, linking further to form a 2D structure by the solvothermal reaction in DMF/HOAc/CH_3OH at 150 ℃ for 90 h (d), and $[Cd_2(CO)_4]$ subunits connected TDPAP to form 1D coordination chains that linked further to form a stair-like 2D structure by the solvothermal reaction in DMF/HOAc/CH_3OH at 150 ℃ for 90 h (e) (Fig. 11).

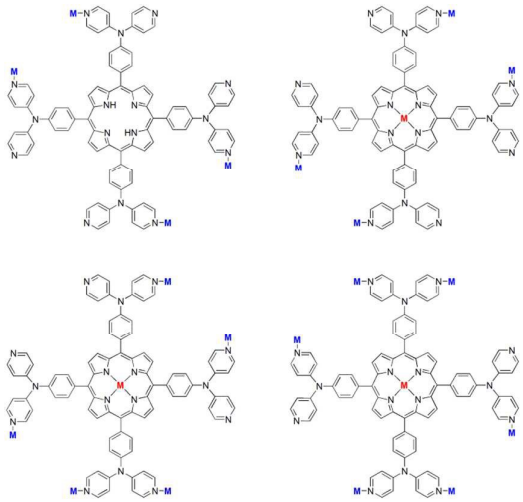

Scheme 3 The coordination modes of TDPAP in 3D frameworks.

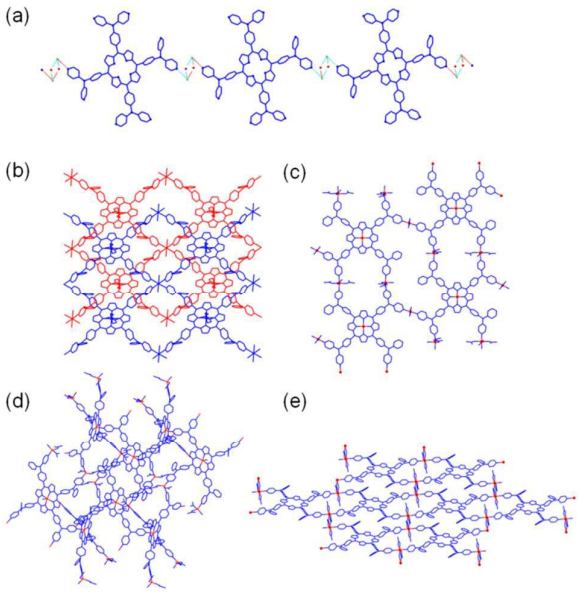

Fig. 11 (a) 1D chain structure formed by intermolecular hydrogen bonds containing $[Cl_2(H_2O)_2]^{2-}$. (b) Interpenetrated 2D networks. (c) 2D network composed of 50- and 70-membered metallomacrocycles. (d) 2D network formed by the linkage of the zigzag chains. (e) 2D network formed by the linkage of 1D chains containing $[Cd_2(CO)_4]$ subunits.

H_2DPyDF5PP (5,15-Dipyridyl-10,20-bis(pentafluorophenyl)-porphyrin)

ZnDPyDF$_5$PP and a designed organic building block, tetratopic 1,2,4,5-tetrakis(4-carboxyphenyl)benzene, provided a noninterpenetrated ZnPO-MOF (a zinc-based, pillared paddlewheel MOF) possessing large pores, permanent microporosity, and a fully reactant-accessible active site for effective catalysis (Fig. 12).[36] Proof-of-concept catalysis of an acyl-transfer reaction between *N*-acetylimidazole (NAI) and 3-pyridylcarbinol (3-PC) revealed ~2420-fold rate enhancement, dominated by contributions from Lewis acid activation and reactant preconcentration in confined spaces. A control experiment catalyzed by a simpler MOF, $Zn_2(1,4\text{-BDC})_2(4,4'\text{-bipyridine})$, where 1,4-BDC is 1,4-benzenedicarboxylate, exhibited very low catalytic activity.

CrystEngComm Accepted Manuscript

This journal is © The Royal Society of Chemistry 20xx

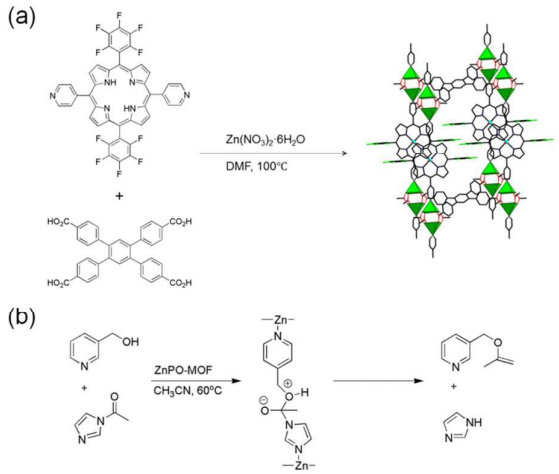

Fig. 12 (a) Preparation of ZnPO-MOF. (b) The acyl-transfer reaction between *N*-acetylimidazole (NAI) and 3-pyridylcarbinol (3-PC).

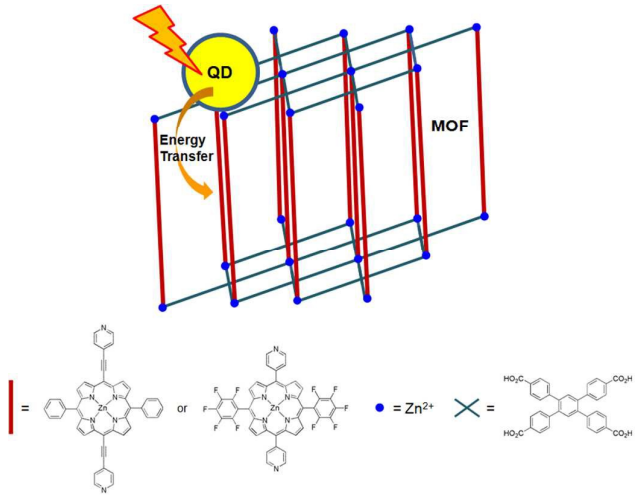

Fig. 13 Illustration of a QD–MOF light-harvesting device. The MOF platelet contains Zn^{II} metal ions connecting 1,2,4,5-tetrakis(4-carboxyphenyl)benzene and dipyridyl porphyrins. The CdSe/ZnS core/shell QDs with a monolayer of amine group-containing polymer are sensitized on the MOF surface through the amine-Zn interactions. The QD-MOF can harvest photons by energy transfer from the QDs to the MOF.

Highly ordered porphyrin ligands in porph-MOFs might be expected to effectively emulate the electron transfer of the organized array of porphyrin-like pigments such as chlorophylls,[4] and antenna-like light-harvesting would then also be possible for use in solar energy conversion. For this purpose, F-MOF and DA-MOF composed of two Zn^{II} porphyrin struts ZnDPyDF$_5$PP and ZnDPyDEPP (H_2DPyDEPP = 5,15-bis[4-(pyridyl)ethynyl]-10,20-diphenylporphin), respectively, were investigated by Farha, Wiederrecht, Hupp, and coworkers.[52] From fluorescence quenching experiments and theoretical calculations, it was revealed that the photogenerated exciton migrates over a net distance of up to ~45 porphyrin struts within its lifetime in DA-MOF (but only ~3 porphyrin struts in F-MOF), with a high anisotropy along a specific direction. Therefore, the exciton diffusion length could be extended by employing a suitable custom-designed porphyrin linker for efficient, light-harvesting, porph-MOF systems. Additionally, the functionalization of porphyrin-based MOFs with CdSe/ZnS core/shell quantum dots (QDs) was reported to enhance the light-harvesting efficiency via energy transfer from the QDs to the MOF by Wiederrecht, Hupp, and coworkers.[53] The broad absorption band of the QDs in the visible region offers greater coverage of the solar spectrum for the new type of QD–MOF hybrid light-harvesting antenna device (Fig. 13).

CrystEngComm Accepted Manuscript

Table 1. Pyridyl-based porph-CPs and porph-MOFs.

Compound	Structure	Ref.
Zn(MTPyP)	1D zigzag chain	12
(PdTPyP)-2Cd(NO_3)·2hydrate	3D	13
Ag:porph 1:1 with Cu^{I}	3D, **PtS**	14
$\{[(MnTPP)]_2(TPyP)(ClO_4)_2\}_\infty$	2D	15
$[M(TPyP)]_6$·G (M = Co^{II}, Mn^{II}, G = $12CH_3COOH·12H_2O$, $60H_2O$, $12C_2H_5OH·24H_2O$) (**SMTP-1**)	3D	16
$[Cu(TPyP)Cu_2Mo_3O_{11}]$ $[Fe(TPyP)_3Fe(Mo_6O_{19})_2]·xH_2O$	3D 3D	17
$[(HgI_2)TPyP]·2TCE$ (TCE=tetrachloroethane) $[(PbI_2)TPyP]·4TCE$ $[(CdI_2)TPyP]·4TCE$ $[(HgI_2)_2Zn_xTPyP]·4TCE$ $[(HgBr_2)TPyP]·6TCE$ $[(HgI_2)_2TPyP]·4TCE$	1D 2D 2D 1D 1D 1D	18
$Hg_2(H_2TPyP)Br_4·2CHCl_3$	1D	19
$[Ag(H_2tpyp)]PF_6·1.5TCE·MeOH·H_2O$	1D chain	20
$2(ZnTPyP)·5(C_6H_5NO_2)$	Ladder type	21
FeTPyP	2D with different packing sequence, ABAB and ABCDABCD	22
$C_{60}·H_2TpyP·Pb(NO_3)_2·1.5TCE$	2D (The fullerenes are intercalated between these layers, acting as pillars.)	23
$[Ag_4(H_2tpyp)_3](NO_3)_4·xSolv$ $[Ag_2(H_2tpyp)(NO_3)](NO_3)_4·xSolv$ $[Ag_8(Zntpyp)_7(H_2O)_2](NO_3)_8·11TCE·17.5DMA·12H_2O$ (DMA= N,N-dimethylacetamide)	2D 2D 3D	24
$[Cu(TPyP)\{Cu_2V_2O_2(O_3PC_6H_5)_4\}]·2H_2O$ $[Ni(TPyP)\{V_4O_4(O_3PC_6H_5)_4\}]·2H_2O$	3D oxide framework	25
$[(AgTrif)_2(H_2Tpyp)]·xSolv$ (Trif = triflate) $[(Ag\{m\text{-}Chla\}_2)_2(H_2Tpyp)](Tos)_2·xSolv$ (Tos= tosylate, m-Chla= m-chloroaniline) $[Ag_2(m\text{-}Tol)(ZnTpyp)_2](Trif)_2·xSolv$ (m-Tol= m-toluidine) $[(AgTos)_2(ZnTpyp·DMA)]·xSolv$	2D	26
$[ZnTPyP]_6$	3D (R-3)	27
$[Zn(TPyP)]·1.6C_2H_4O_2$	3D (R-3)	28
$[Zn(TPyP)]_\infty$	1D ribbon	29
$H_2T(3\text{-}Py)P·HgI_2·C_{60}$	2D (fullerene – porphyrin framework)	30
$[Cu_2(AcO)_4(CuTPyP)_{1/2}]·CHCl_3$	2-D square-grid	31
$\{Cd(TPyP)·C_6H_5N\}$ $\{Cd(H_2TPyP)(SH)_2\}$ $\{Cd(TPyP)·CdI_2\}$ $\{Cd_3(TPyP)_2(SCH_2CH_2OH)_2·2DMF\}$	0D 3D, $CdSO_4$ type 3D, **hms** 2D	32
$[\{cis\text{-}(dppf)Pt\}_{12}(TPyP)_6](OTf)_{24}$ (dppf =1,1'-bis(diphenylphosphino)-ferrocene, OTf = $CF_3SO_3^-$)	0D, open molecular box	33
Co-PyTIPP Zn-PyTIPP Zn-DPyDIPP	0D 2D 3D	34
Zn-PyDXPP (X = OCH_3, OH) Zn-DPyDCF$_3$PP	3D 1D	35
$[Zn_2(ZnDPyDF_5PP)(TCB)]_n$ (**ZnPO-MOF**)	3D	36
$ZnTPyP·ZnCl_2·3C_2H_2Cl_4$	2D, grid	37
$[(HgI_2)_2TPyP]·4TCE$ $[(ZnBr_2)_2TPyP]·6TCE$ $[(MnCl_2)TPyP]·6TCE$	1D chain 1D chain 2D square grid of (4,4) type	38
$\{[Nd(NO_3)_3(H_2O)_2]·TPyP·3(o\text{-}DCB)\}$ (o-DCB = o-dichlorobenzene) $\{[Sm(NO_3)_3(H_2O)_2]·TPyP·3(o\text{-}DCB)\}$ $\{[Gd(NO_3)_3(H_2O)_2]·TPyP·3(o\text{-}DCB)\}$ $\{[Tb(NO_3)_3(H_2O)_2]·TPyP·3(o\text{-}DCB)\}$ $\{[Dy(NO_3)_3(H_2O)_3]·TPyP·2(benzene)\}$ $\{[Yb(NO_3)_3(H_2O)_3]·TPyP·2(benzene)\}$ $\{[Yb(NO_3)_3(H_2O)_3]·TPyP·2(o\text{-}DCB)\}$ $\{[La(NO_3)_5(EtOH)]^{2-}·(H_2T(3\text{-}Py)P)^{2+}·(o\text{-}DCB)\}$ $\{[Dy(NO_3)_3(H_2O)_2(EtOH)]·TPyP·3(o\text{-}DCB)\}$ $\{[Sm(NO_3)_4(H_2O)_2]^-·(HTPyP)^+·31/2(o\text{-}DCB)\}$ $\{[Yb(NO_3)_3(H_2O)_2(EtOH)]·TPyP·3(o\text{-}DCB)\}$	3D intermolecular connectivity pattern sustained by hydrogen bonding	39
$(ZnTPyP)_4$ cyclic tetrameric oligomer ZnTPyP	0D 2D, square grid	40
$CuTPyP·Cu(hfacac)_2$	2D sheet, distorted (4,4) net	41
$[ZnX_2(\mu_3\text{-}ZnTPyP)·3TCE]_n$ (*X* = Cl, Br)	2D, grid	42
ZnT(3-Py)P (**MPF-3**)	2D, tessellation	43
$Sn^{IV}Cl_2$-T(3-Py)P complex Cu^{II}T(3-Py)P Cu^{II}T(3-Py)P· $(Cu^{I}Cl)_4$ Cu^{II}T(3-Py)P· $(Cu^{I}I)_4$ $[(Mn^{II}T(3\text{-}Py)P)_2·(Mn^{IV}Cl_2T(3\text{-}Py)P)·[Mn^{III}Cl_3·Mn^{II}Cl_2]$ $Mn^{II}(DMF)_2T(3\text{-}Py)P$ $T(3\text{-}Py)P·2[Yb^{III}(NO_3)_3(H_2O)_2(EtOH)]$· o-DCB $(H_4T(3\text{-}Py)P)^{4+}·2[Yb^{III}(NO_3)_4(H_2O)_2^-]·2(NO_3^-)$ $(H_2T(3\text{-}Py)P)^{2+}·[Ce(NO_3)_5·(EtOH)^{2-}]$·o-DCB	0D 1D 3D 3D 3D 3D H-bonded 3D H-bonded 3D H-bonded 3D	44
CoT(3-Py)P CoT(3-Py)P·2DMF $CdCl_2·H_2T(3\text{-}Py)P$ $CdCl_2T(3\text{-}Py)P$ Cd(DMF)T(3-Py)P $(Cu^{I}Br)_4·CuT(3\text{-}Py)P$	2D 2D 3D diamondoid 3D chair-like 3D 3D	45
$CdI_2·TPyP$ (**HMOF-1**)	3D, **cds** type	46
$[Zn_2(H_2O)_4Sn^{IV}(TPyP)(HCOO)_2]·4NO_3·DMF·4H_2O$	3D	47
CuTPyP nanoplates to microspindles	2D	48
$\{[Cd(DMF)_2Mn^{III}(DMF)_2TPyP](PW_{12}O_{40})\}·2DMF·5H_2O$ (unique layered polyoxometalate-Mn^{III}-metalloporphyrin based hybrid material)	Layer	49
CuTPyP, CuDPyP on Au(111)	2D	50
$H_4TDPAPCl_2·2CH_3OH·2H_2O$ $[Mn^{III}Mn^{II}(TDPAP)Cl_3(DMF)]_n$ $[Cu_4(TDPAP)(CH_3COO)_5(HCOO)(CH_3COOH)(H_2O)_3]_n·nCH_3COOH·nH_2O$ $[Zn_3(TDPAP)(CH_3COO)_4]_n$ $[Cd_2H_2(TDPAP)(CH_3COO)_4]_n·nDMF·nCH_3COOH·2nH_2O$	1D 2D → 3D 2D 1D → 2D 2D	51
Zn($DPy\ DF_5PP$)·Zn(TCB) (**F-MOF**) Zn(DPyDEPP)·Zn(TCB) (**DA-MOF**)	3D 3D	52

CrystEngComm Accepted Manuscript

This journal is © The Royal Society of Chemistry 20xx

F-MOF **DA-MOF**		53
[Mn(TPyP)OAc] supported on silica-coated magnetite nanoparticles, Fe_3O_4-SiO_2		54
Cu(ZnTPyP) nanosheet	2D	55
$[H_4Zn(TPyP)(H_2O)]^{4+}(NO_3)_4(CH_4O)(H_2O)_2$ $\{[Zn(TPyP)]\cdot CH_4O\cdot(H_2O)_2\}_n$	0D, complex 3D, (R-3)	56
$Co_3(DPyP)_3\cdot 4DMF$ $Zn_3(DPyP)_3\cdot 2DMF\cdot 4H_2O$	1D 1D	57
$[Co(DPyDtolP)]_6\cdot 12H_2O$	3D (R-3)	58
$[Co(DPyDCNPP)]_6\cdot 18H_2O$ $[Co(DPyDClPP)]_6\cdot 18H_2O$	3D (R-3)	59

Carboxyphenyl-based porphyrinic MOFs

Carboxy-based porphyrin ligands used in the construction of porphyrinic frameworks are listed in Scheme 4, and Table 2 summarizes the porph-CPs and porph-MOFs containing carboxy-based porphyrins.[60-135]

Tetrakis(carboxyphenyl)porphyrins: H_6TCPP (5,10,15,20-tetrakis(4-carboxyphenyl)porphyrin)

Porph-MOFs containing TCPP (5,10,15,20-tetrakis(4-carboxyphenyl) porphyrinato) bridging ligand have been addressed by Goldberg,[60-63,65,67-69,72-75,77,114] Suslick,[64,66,70] Choe,[78-82,84,92,102] Hupp,[91,93,115,133] Zhou,[99,117-119,126,130,132] Wu,[88,101,108,113,116,124] Ma,[94,98,100,103,107,111,112,123] Kitagawa,[86,87,96,109,121] and others,[71,83,89,90,95,97,104-106,110,128,129,131,134] considering many reviews and literatures.[7-10]

PIZA (porphyrinic Illinois zeolite analogue) series were synthesized with Co^{II} and Mn^{II} metalloporphyrin frameworks containing TCPP, showing remarkable size selectivity for small-molecule sorption and capability of oxidation catalysts; however, due to the very small channels, catalysis of the substrates examined occurs only on the exterior surface.[64,70]

CrystEngComm Accepted Manuscript

CrystEngComm

HIGHLIGHT

Scheme 4 Carboxyphenyl-based porphyrin ligands for porph-MOFs. H_6TCPP = 5,10,15,20-tetrakis(4-carboxyphenyl)porphyrin; H_6T*m*CPP = 5,10,15,20-tetrakis(*m*-carboxyphenyl)porphyrin; H_6TCBPP = 5,10,15,20-tetrakis(4-carboxybiphenyl)porphyrin; H_6TCPEP = 5,10,15,20-tetrakis(4-carboxyphenyl)ethynylporphyrin; H_6TCP series = tetrakis(4-carboxyphenyl)porphyrin, elongated with desired conformation by arranging the vicinal phenyl ring and carboxylate group; H_6TCMOPP = 5,10,15,20-tetrakis[4-(carboxymethyleneoxy)phenyl]porphyrin; *cis*-H_4DCPP = 5,10-di(4-carboxyphenyl)-15,20-diphenylporphyrin; *trans*-H_4DCPP = 5,15-di(4-carboxyphenyl)-10,20-diphenylporphyrin; H_{10}TDCPP(H_{10}OCPP) = 5,10,15,20-tetrakis(3,5-dicarboxyphenyl)porphyrin (= octacarboxyphenylporphyrin); H_{10}TDCBPP = 5,10,15,20-tetrakis(3,5-dicarboxybiphenyl)porphyrin; H_{10}TBCPPP = tetrakis{3,5-bis[(4-carboxy)phenyl]phenyl}porphine; H_6BDCPP = 5,15-bis(3,5-dicarboxyphenyl)porphyrin; H_6BCDBP = 5,15-bis(3,5-dicarboxyphenyl)-10,20-bis(2,6-dibromophenyl)porphyrin; and H_6BDCBPP = 5,15-bis(dicarboxybiphenyl)porphyrin.

CrystEngComm Accepted Manuscript

Please do not adjust margins

CrystEngComm

HIGHLIGHT

Porphyrin paddlewheel frameworks (PPF series) were synthesized using metalloporphyrins and paddlewheel SBUs, and these 2D porphyrinic layers were further interconnected by dipyridyl pillaring linkers to form 3D frameworks[76,78,79,81,82,92,102] (Fig. 14). A systematic study of PPF series was independently addressed by Choe, Ma, Wu and coworkers.[9-11] Choe and coworkers reported the construction of a 3D framework from a 2D bilayer framework in an overall three-step self-assembly,[92] and they also showed bridging-linker replacement in extended 2D and 3D MOFs by introducing pillared paddlewheel MOF structures into a solution containing dipyridyl linkers through a single-crystal-to-single-crystal transformation.[93]

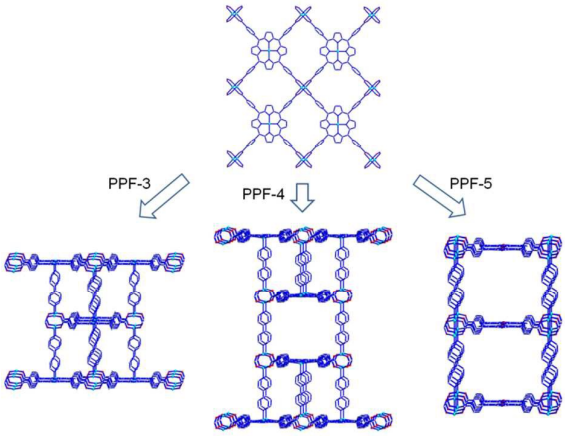

Fig. 14 Stacking control of porphyrin framework series, PPF-3, PPF-4, and PPF-5 synthesized by the solvothermal reaction in DMF/ethanol for 24 h.

A series of porous metal–metalloporphyrin frameworks (MMPFs) were reported by Ma and coworkers.[94,98,100,103,107,111,112,123] MMPFs compose a class of coordination networks self-assembled using metal-containing SBUs and custom-designed metalloporphyrin ligands. Among MMPFs, only MMPF-6 was based on an FeCl(TCPP) ligand and an SBU of a zirconium oxide cluster; other MMPFs contained custom-designed metalloporphyrin ligands, which will be described later. MMPF-6 was formed by the solvothermal reaction of zirconyl chloride octahydrate ($ZrOCl_2 \cdot 8H_2O$) and FeCl(TCPP) in DMF/formic acid at 135 ℃ for 80 h and demonstrated interesting peroxidase activity comparable to that of the heme protein myoglobin and exhibited solvent adaptability of retaining peroxidase activity in an organic solvent (Fig. 15).[107]

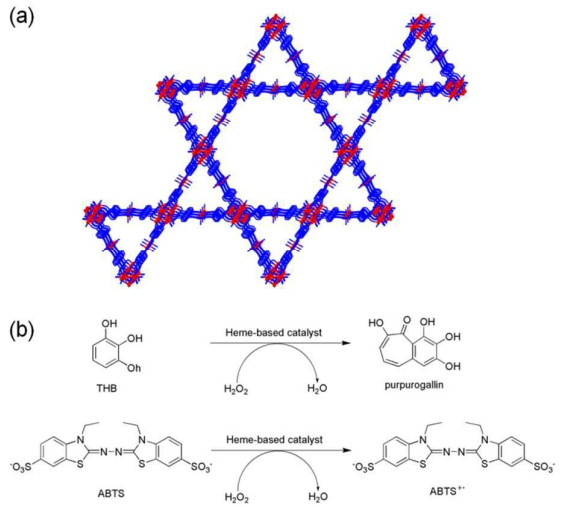

Fig. 15 (a) Hexagonal and triangular 1D channels of MMPF-6 with a Kagomé-like net. (b) Oxidation reactions of 1,2,3-trihydroxybenzene (THB) and 2,2′-azinodi(3-ethylbenzothiazoline)-6-sulfonate (ABTS) with hydrogen peroxide catalyzed by a heme-based catalyst.

Wu and coworkers reported a functionalized MOF assembled by the thermal reaction of Pd-H_4TCPP and $Cd(NO_3)_2 \cdot 4H_2O$ in DMF/CH_3OH/acetic acid at 80 ℃ for ten days, which presents 3D framework with high stability and interesting catalytic ability for the selective oxidation of styrene (Fig. 16a).[88] They used a series of TCPP ligands and Pb^{II} cations to construct five interesting coordination networks. The conformations of the porphyrin rings range from flat to wavy to bowl-shaped, and the diverse porphyrin cores play an important role in the stacking of the porphyrin rings.[101] Chen and Wu et al. also succeeded in preparing a porous Mn^{III}-porphyrin MOF (CZJ-1, Chemistry Department of Zhejiang University) by the thermal reaction in DMF/ethanol at 80 ℃ for two days with highly efficient oxidative C-H bond activation (Fig. 16b).[113] Wu and Ma et al. reported metalloporphyrinic frameworks formed from Mn^{III}Cl-TCPP and M' (Zn^{II} or Cd^{II}) nitrate by the thermal reaction in DMF/acetic acid at 80 ℃ for five days, and they can be used as heterogeneous catalysts for selective oxidation and aldol reactions (Fig. 16c).[116]

CrystEngComm Accepted Manuscript

Please do not adjust margins

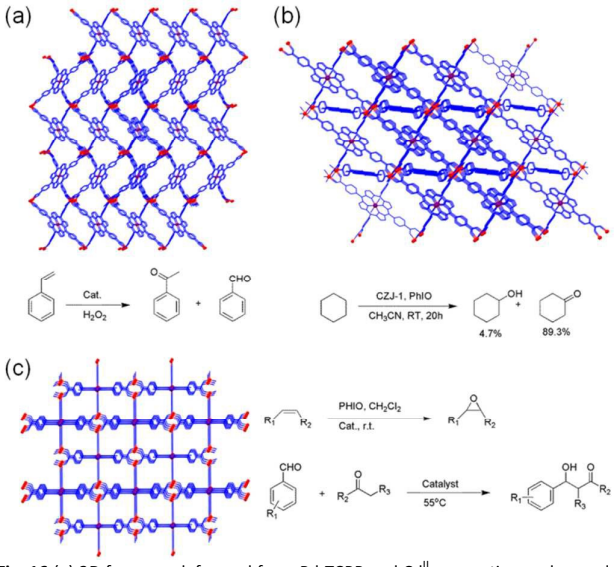

Fig. 16 (a) 3D framework formed from Pd-TCPP and Cd^{II} connecting nodes, and selective oxidation of styrene catalyzed by Cd(Pd-TCPP) MOF. (b) Crystal structures of CZJ-1, and selective oxidation of cyclohexane catalyzed by CZJ-1. (c) 3D porphyrinic framework; selective epoxidation of olefins and aldol reaction of aldehydes and ketones catalyzed by M′(MnCl-TCPP) MOF.

A series of porph-MOFs containing TCPP was prepared by Fateeva and coworkers from the reaction between $FeCl_3 \cdot 6H_2O$ and H_6TCPP in the presence of different bases.[134] Depending on the conditions, permanently microporous porph-MOFs with **pts**, **pcu-b** and **fry** topology were prepared.

PCN series (PCN = porous coordination network) containing TCPP or MTCPP (M = Mn^{III}, Fe^{III}, Co^{II}, Ni^{II}, Cu^{II}, or Zn^{II}) and Zr^{IV} clusters were reported by Zhou and coworkers. Generally, MOFs containing Zr^{IV} oxo-cluster-based SBUs found in the UiO-66 family exhibited inherently higher hydrolytic stability compared with other MOFs. Solvothermally prepared PCNs are 3D heme-like MOFs with mesopores, accessible redox sites, and ultrahigh stability, especially in aqueous media.[99,117-119,126,130,132] A highly stable, mesoporous MOF PCN-222(Fe) showed biomimetic catalytic activity, and the active site of the catalyst is located on the inner wall of an open channel with a diameter of 3.7 nm, showing good activity for the oxidation of a variety of substrates.[99] Zr-PCN-221(M) and Hf-PCN-221(M) (M = Fe^{III}, Cu^{II}, Co^{II}, or no metal) with a (4,12)-connected **ftw** topology exhibited high surface areas, gas uptakes, and catalytic selectivity for cyclohexane oxidation.[117] PCN-225 and PCN-225(Zn) with a (4,8)-connected **sqc** net exhibited exceptional chemical stability in aqueous solutions with a pH ranging from 1 to 11, and PCN-225(Zn) has potential in a variety of applications, especially catalysis, light-harvesting, and sensors.[118] PCN-224 with a (4,6)-connected **she** net possesses 3D channels as large as 19 Å and exhibits high stability over a wide pH range in aqueous solution, and PCN-224(Co) showed very high efficiency as a heterogeneous catalyst in the coupling reaction of CO_2 and epoxide with good recyclability (Fig. 17a).[119] A series of mesoporous metalloporphyrin PCN-600(M) (M = Mn^{III}, Fe^{III}, Co^{II}, Ni^{II}, or Cu^{II}) have been prepared, and a mesoporous MOF PCN-600(Fe) with exceptional chemical stability and extraordinary porosity has been demonstrated as an effective peroxidase mimic to catalyze the co-oxidation reaction on the active site inner wall of a 3.1-nm 1D channel.[126] PCN-223, the first example of a (4,12)-connected **shp**-**a** network, was constructed from the newly reported hexagonal prismatic 12-connected Zr_6 cluster, showing high stability in aqueous solutions with a wide pH range, and cationic PCN-223(Fe) formed by postsynthetic treatment was an excellent recyclable heterogeneous catalyst for the hetero-Diels-Alder reaction (Fig. 17b).[130]

Harris and coworkers metallated PCN-224 with Fe^{II} to yield a 4-coordinate ferrous heme-containing compound, and the heme center binds O_2 at -78 °C to give a 5-coordinate heme-O_2 complex, which was unequivocally characterized by X-ray crystallography.[128] Yaghi and coworkers also synthesized MOF-525, MOF-535, and MOF-545 based on two new topologies, **ftw** and **csq**, and they were exceptionally chemically stable, maintaining their structures under aqueous and organic conditions. MOF-525 and MOF-545 were metallated with Fe^{III} and Cu^{II} to yield the metallated analogues without losing their high surface areas or chemical stability.[106]

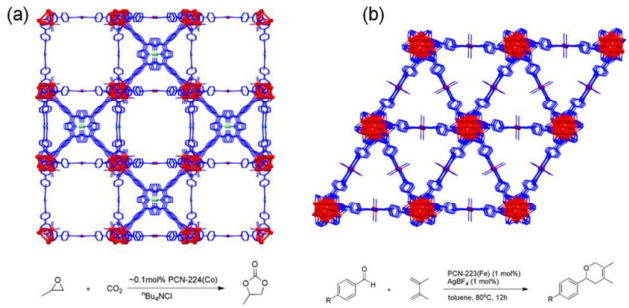

Fig. 17 (a) Crystal structure of PCN-224(Ni) containing the 6-connected D_{3d}-symmetric Zr_6 and the CO_2 and propylene oxide coupling reaction catalyzed by PCN-224(Co). (b) Crystal structure of PCN-223(Fe), and the hetero-Diels-Alder reaction catalyzed by PCN-223(Fe).

The free-base PCN-222/MOF-545 Zr^{IV}-based porph-MOF containing H_2TCPP bridging ligands was prepared and utilized as a heterogeneous photooxidation catalyst for the transformation of a mustard-gas simulant, 2-chloroethyl ethyl sulfide (CEES), into 2-chloroethyl ethyl sulfoxide (CEESO).[133] The reactive singlet oxygen species ($^1O_2$) was produced through sensitization by PCN-222/MOF-545 under the irradiation of a commercially available light-emitting diode.

Similar CPs containing MTCPP and bridging metal ions or metal clusters have been studied by several research groups.[71,83,89,97,104]

Controlling the size and growth direction of MOFs or PCPs at the nanoscale is a critical issue for their potential activity applications. Kitagawa and coworkers discussed several approaches to employing metalloporphyrin-based components to build multidimensional nanoarchitectures.[86,11] Bottom-up fabrication protocols are highly suitable for extension to the formation of quasi-infinite nanostructures on surfaces (NAFS-1, nanofilm of MOFs on surface no. 1).[87] Layer-structured MOF nanofilms (NAFS-2) consisting of

CrystEngComm Accepted Manuscript

This journal is © The Royal Society of Chemistry 20xx

Please do not adjust margins

H_2TCPP and Cu^{II} ions were assembled on gold or silicon surfaces by applying a solution-based layer-by-layer (LbL) growth technique coupled with the Langmuir-Blodgett (LB) method,[96] and their thermal stability is a key issue for the future use of MOFs in potential applications in nanodevices. They also reported MOF thin films with perfect orientation and excellent crystallinity formed from nanosheet-structured components, CuTCPP, by a new "modular assembly" strategy.[109] They fabricated the pre-synthesized MOF nanosheets (CuTCPP) on the surface of certain electrodes, forming LbL nano-thin films.[121]

Farha, Hupp, and coworkers also reported two thin films (DA-MOF and L2-MOF) of porph-MOFs on functionalized surfaces using an LbL technique.[122] Morris and coworkers recently reported a thin film of a metalloporphyrin MOF consisting of CoTCPP struts bound by linear trinuclear Co^{II}-carboxylate clusters on electrically conducting fluorine-doped tin oxide glass (CoPIZA/FTO), and this CoPIZA/FTO provided large cavities and access to metal active sites, revealing an electrochemically active material.[131]

In situ esterification of porphyrin: H_2TCPP-Et_4 and TCPP-Me_4

Chen and Fukuzumi reported a series of metalloporphyrins, M(TCPP-Et_4) (M = Zn^{II}, Cu^{II}, or Ni^{II}; Et = CH_2CH_3), M(TCPP-Me_4) (M = Zn^{II}, Cu^{II}, or Co^{II}; Me = CH_3), and two nonmetallated compounds, H_2TCPP-Et_4 and H_2TCPP-Me_4·H_2O. These compounds were prepared by solvothermal reactions in ethanol or methanol at 180 ℃ for 1 day, and Zn(TCPP-Me_4) was characterized as a 2D CP possessing a large void space (361 $Å^3$, 14% of the unit-cell volume) (Fig. 18).[83] They revealed that in situ esterification of the carboxylic acid groups in the TCPP ligand not only induced different structural motifs and supramolecular networks but also changed the properties of the compounds.

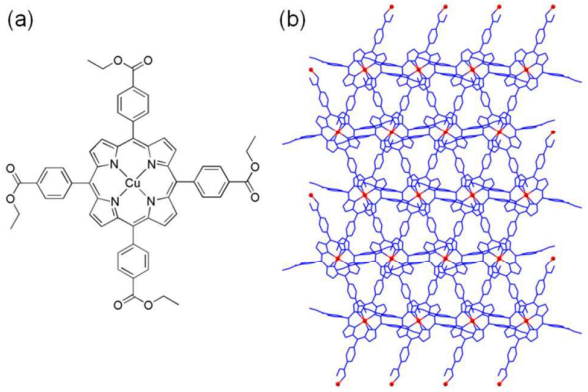

Fig. 18 (a) Chemical structure of Cu(TCPP-Et_4). (b) 2D structure of Zn(TCPP-Me_4).

Tetrakis(*m*-carboxyphenyl)porphyrin: H_6T*m*CPP (5,10,15,20-tetrakis(*m*-carboxyphenyl)porphyrin, also called H_6T^3CPP)

Goldberg and coworkers reported porph-MOFs assembled from the reactions of H_6T*m*CPP (Scheme 3) and MTCPP with lanthanoid salts.[75] The "hard" lanthanoid ions tend to form polynuclear units bridged by several anions. Goldberg and coworkers succeeded in constructing lanthanoid-T*p*CPP (usually called TCPP) CPs,[73,74] and they also focused on the tessellation of CPs containing T*m*CPP and lanthanoid ions, which are characterized by a different direction of coordination modes due to the *meta*- rather than *para*-disposition of the carboxylate groups of the phenyl rings.[75] Goldberg and coworkers also reported conformations of 3-carboxylate substituents on the porphyrin core: chair- and table-like conformations (Fig. 19).[114] In the chair-like conformer of T^3CPP, two adjacent carboxylate groups are oriented upward and the other two downward, and in the table-like conformer, all four carboxylate groups are oriented in the same direction. The hydrogen-bonding networks revealed the chair-like conformer of the $[T^3CPP]^{2-}$ ion, and the table-like conformer was obtained in coordination compounds with Zn^{II} and Cd^{II} ions.

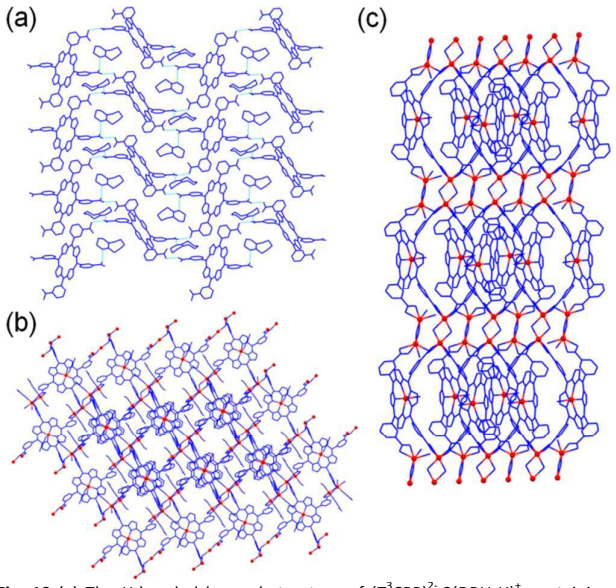

Fig. 19 (a) The H-bonded layered structure of $(T^3CPP)^{2-}\cdot2(DBU\text{-}H)^+$ containing the chair-like conformer of the $[T^3CPP]^{2-}$ ion (DBU = 1.8-diazabicyclo[5.4.0]undec-7-ene). (b) The bilayered structure of $\{[Cd(DMF)T^3CPP]^{4-}\cdot[Cd(DMF)(MeOH)Cd(DMF)]^{4+}\}$ containing the table-like conformer of T^3CPP. (c) Bilayered coordination patterns of the tube-like polymeric metal-porphyrin arrays of $\{[Cd(DMF)T^3CPP]^{4-}\cdot4(CdCl)^+\}$.

Tetrakis(carboxybiphenyl)porphyrins: H_6TCBPP (5,10,15,20-tetrakis(4-carboxybiphenyl)porphyrin), H_6TCPEP (5,10,15,20-tetrakis(4-carboxyphenyl)ethynylporphyrin), H_6TCP series (tetrakis(4-carboxyphenyl)porphyrin), elongated with the desired conformation by arranging the vicinal phenyl ring and carboxylate group)

Two rare In^{III}-based porph-MOFs, MMPF-7 and MMPF-8 possessing the **pts** topology, were constructed by the solvothermal reactions of In^{III} ions and two custom-designed porphyrin-tetracarboxylate ligands (TCPP and TCBPP) in DMF at 85 ℃ for 48 h. MMPF-8 exhibited a N_2 uptake capacity of ~150 $cm^3\ g^{-1}$ at 1 atm, whereas MMPF-7 did not show N_2 sorption at 77 K due to its smaller pore size. Both MOFs also

CrystEngComm Accepted Manuscript

displayed CO_2 adsorption properties depending on the pore size (Fig. 20a).[111]

Matsunaga, Mori, and coworkers designed a new tetracarboxyporphyrin building block, ZnTCPEP-H_4, with an acetylene moiety between the carbon atom at the *meso*-position and the 4-carboxyphenyl group and used it in the construction of a new porph-MOF, $[Zn_4(\mu_3\text{-}OH)_2(H_2O)_2(ZnTCPEP\text{-}H)_2(DABCO)]\cdot 2DMF\cdot 10.5H_2O$ (Zn_4·ZnTCPEP·DABCO), which forms a 3D network linked by tetranuclear Zn cluster nodes $\{Zn_4(\mu_3\text{-}OH)_2(H_2O)_2\}$, ZnTCPEP-$H_4$, and DABCO (Fig. 20b).[90] The porph-MOF had a Brunauer-Emmett-Teller (BET) surface area of 461 $m^2\ g^{-1}$ with a Type I adsorption isotherm.

A series of Zr_6-containing isoreticular porph-MOFs, PCN-228, PCN-229, and PCN-230, containing TCP-1, TCP-2, and TCP-3 with **ftw-a** topology were synthesized with the solvothermal reaction in DMF at 120 ℃ for 12 h by Zhou and coworkers (Fig. 20c), and PCN-229 demonstrated the highest porosity and BET surface area among the previously reported Zr-MOFs.[132] PCN-230, constructed with the most extended porphyrinic linker, showed excellent stability in aqueous solutions with pH values ranging from 0 to 12 and demonstrated one of the highest pH tolerances among all porph-MOFs.

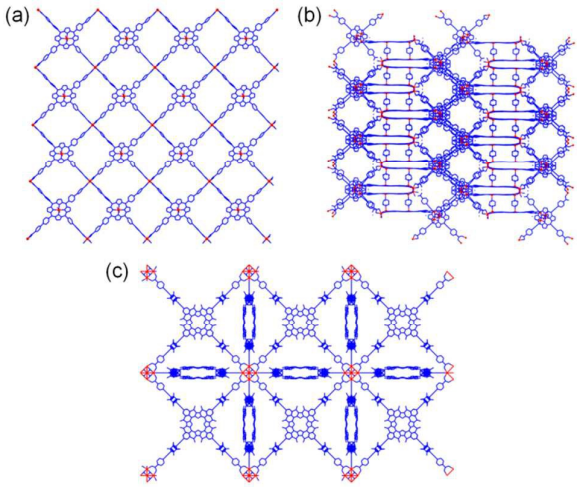

Fig. 20 (a) Structure of MMPF-8. (b) 3D extended structure of Zn_4·ZnTCPEP·DABCO along (a, b) the diagonal line of the *ab*-plane. (c) Structure of PCN-230 constructed with Zr_6 clusters and H_4TCP-3 with space group *Pm*-3*m*.

Bu, Feng, and coworkers reported CPM-99X (CPM = crystalline porous material; X = H_2, Zn, Co, or Fe) porph-MOFs with TCBPP.[135] The pyrolysis of CPM-99Fe at 700 °C gave a porous carbon material, CPM-99Fe/C, containing both porphyrinic active sites and hierarchical porosity. CPM-99Fe/C exhibited good oxygen reduction reaction (ORR) activity, comparable to the commercially available 20 wt% Pt/C catalyst.

Flexible tetra-acids: H_6TCMOPP (tetrakis[4-(carboxymethyleneoxy)phenyl]porphyrin)

Goldberg and coworkers used a flexible tetraacid ligand, H_6TCMOPP, as a new attractive building block for the construction of CPs and hydrogen-bonding supramolecular assemblies in the solid state (Fig. 21).[85]

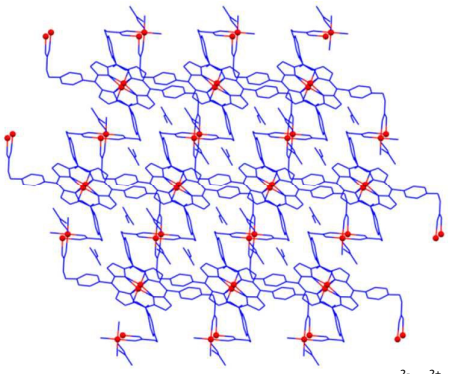

Fig. 21 Thermally prepared 2D layered network of $Zn(TCMOPP)^{2-}Zn^{2+}$ containing paddlewheel-type coordination polymerization. The DMF species coordinated to the Zn^{II} ions and those accommodated in the interface between adjacent layers.

Dicarboxyphenylporphyrins: *cis*-H_4DCPP (5,10-di(4-carboxyphenyl)-15,20-diphenylporphyrin) and *trans*-H_4DCPP (5,15-di(4-carboxyphenyl)-10,20-diphenylporphyrin)

Choe and coworkers reported a novel MOF, PPF-6, [(Co(*cis*-ZnDCPP)(4,4'-bpy)]·4DMF·H_2O (*cis*-ZnDCPP = zinc 5,10-di(4-carboxyphenyl)-15,20-diphenylporphyrin; 4,4'-bpy = 4,4'-bipyridyl) exhibiting CdI_2–type **kgd** 2D layers constructed from paddlewheel building units, $Co_2(COO)_4$, *cis*-ZnDCPP, and 4,4'-bpy linkers (Fig. 22a).[76] They also reported a porphyrin paddlewheel framework (PPF-25), assembled from a Zn^{II} paddlewheel cluster and mixed linkers, 4,4'-bpy and Zn(*trans*-DCPP) (Fig. 22b).[82] The PPF-25 was synthesized by the solvothermal reaction in DMF/ethanol at 80 ℃ for 24 h, and it adopts a (3,6)-connected net with anatase (**ant**) topology. The paddlewheel SBUs act as a six-connected octahedral node, and the Zn(*trans*-DCPP) adopts a T-shaped geometry, forming a rare **ant** topology.

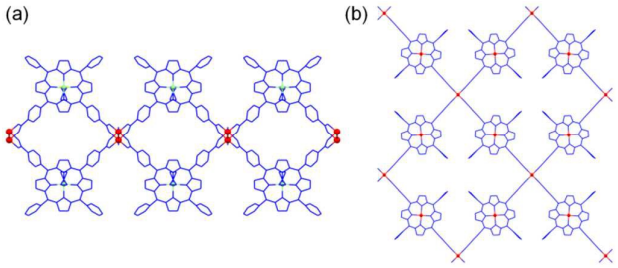

Fig. 22 (a) 1D tape motif assembled from cobalt paddlewheels and *cis*-ZnDCPP for PPF-6. (b) 2D porphyrinic (4,4) grids assembled from *trans*-DCPP for PPF-25.

A Zn_4O SBU with Zn^{II}-(*p*-CO_2)P_2Mes_2P (PIZA-4) ((*p*-CO_2)P_2Mes_2P = 5,15-di(*p*-carboxyphenyl)-10,20-di(2',4',6'-trimethylphenyl)porphyrinate) was synthesized by slow diffusion of trimethylamine vapor into a solution of Zn^{II}-(*p*-CO_2)P_2Mes_2P and $Zn(NO_3)_2$, and it is an interpenetrated 3D framework whose carboxylates coordinate the six edges of tetrahedral Zn_4O^{6+} clusters, maintaining a charge-neutral framework.[66]

CrystEngComm Accepted Manuscript

This journal is © The Royal Society of Chemistry 20xx

Lin and coworkers reported the rational design of a sub-100-nm nanoscale Hf-porph-MOF (NMOF), DBP-UiO ($Hf_6(\mu_3\text{-}O)_4(\mu_3\text{-}OH)_4(DBP)_6$, DBP = 5,15-di(4-benzoato)porphyrinato), as an exceptionally effective photosensitizer for photodynamic therapy (PDT) of resistant head and neck cancers.[129] DBP-UiO was synthesized by the solvothermal reaction between $HfCl_4$ and H_4DBP in DMF at 80 ℃. PDT is an effective anticancer treatment that uses photosensitizers localized near tumor cells. Light activation of the localized photosensitizers generates cytotoxic reactive singlet oxygen species ($^1O_2$) that can effectively disrupt tumor cells. DBP–UiO, a porph-MOF possessing UiO-type structure, is thought to efficiently generate $^1O_2$ from the site isolation of porphyrin ligands in the framework and the enhanced intersystem crossing by heavy Hf centers. Additionally, facile $^1O_2$ diffusion through porous DBP–UiO nanoplates was an important factor in the high PDT effect (Fig. 23). DBP–UiO exhibited greatly enhanced PDT efficiency both *in vitro* and *in vivo*. Half of the mice treated by a single DBP–UiO dose and a single light exposure indicated almost complete tumor eradication. Thus, NMOFs are thought to be a new class of highly effective PDT agents and can be utilized in treating resistant cancers. They also determined the single-crystal structure of an analogue of DBP–UiO, $Zr_6(\mu_3\text{-}O)_4(\mu_3\text{-}OH)_4(Zn\text{–}DPDBP)_6$ (Zn–DPDBP–UiO, DPDBP is 5,15-di(4-benzoato)-10,20-diphenylporphyrinato possessing the same length as H_2DBP) (Fig. 23).

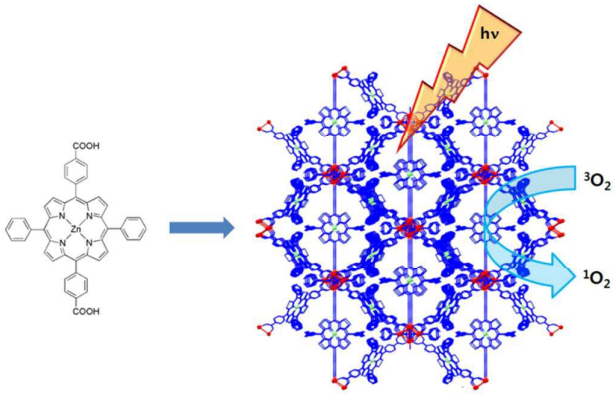

Fig. 23 Structure of Zn-DPDBP-UiO and schematic description of the singlet oxygen generation process.

Octacarboxyphenylporphyrins: H_{10}TDCPP (tetrakis(3,5-dicarboxyphenyl)porphyrin, also called H_{10}OCPP (octacarboxyphenylporphyrin or 5,10,15,20-tetrakis(3,5-biscarboxylphenyl)porphyrin)), H_{10}TDCBPP (5,10,15,20-tetrakis(3,5-dicarboxybiphenyl)porphyrin), and H_{10}TBCPPP (tetrakis{3,5-bis[(4-carboxy)phenyl]phenyl}porphine)

Ma et al. reported a MMPF-2 constructed from a custom-designed octatopic porphyrin ligand, TDCPP that links a distorted Co^{II} trigonal prism SBU (Fig. 24a).[100] MMPF stands for metal–metalloporphyrin framework. MMPF-2 was synthesized by the solvothermal reaction of H_{10}TDCPP and $Co(NO_3)_2{\cdot}6H_2O$ in dimethylacetamide (DMA) at 115 ℃. They also reported MMPF-4 and MMPF-5, and MMPF-4 exhibits high surface areas and adsorption selectivity for CO_2 over N_2. Considering the high symmetry of small cubicuboctahedron SBUs, MMPF-4/5 may serve as a blueprint for the design of a range of highly porous MOFs (Fig. 24b).[103] MMPF-5(Co) was prepared as a metalloporphyrin-based nanoreactor by post-synthetic metal-ion exchange of the catalytically inactive Cd^{II} ion at the porphyrin center in MMPF-5, consisting of nanoscopic cubicuboctahedral cages from the immersion of MMPF-5(Cd) in Co^{II} cations.[112] MMPF-5(Co) preserved its permanent microporosity and showed good catalytic activity in the epoxidation of *trans*-stilbene.[112] The exchange of metal ions within porphyrin rings without losing single crystallinity or permanent porosity of a framework suggests an easy way to create porph-MOFs with different active centers in the same framework structure to tailor heterogeneous porph-MOF catalysts on demand.

Chen, Wu, and coworkers incorporated M-H_8OCPP into porous MOFs (ZJU-18, ZJU-19, ZJU-20; ZJU = Zhejiang University) that displayed highly efficient and selective catalytic oxidation of alkylbenzenes, which were examined at 65 °C using *tert*-butyl hydroperoxide (TBHP) as the oxidant (Fig. 24c)[108] ZJU-18 and ZJU-19 were synthesized by the thermal reactions in DMF/acetic acid at 80 ℃ for a week. Two porous mixed-metal metal–organic frameworks (M'MOFs), ZJU-21 and ZJU-22, containing nanoporous cages (2.1 nm in diameter) or nanotubular channels (1.5 nm in diameter) were synthesized by the thermal reactions in DMF/dilute HNO_3 at 65 ℃ for a week, and the heterogeneous catalytic activities of ZJU-21 and ZJU-22 are remarkable: (1) their efficiency is comparable to those of their homogenous counterparts, (2) no auxiliary agent is required, and (3) the reaction is environmentally friendly.[124] In ZJU-22, highly reactive Cu^{2+} sites are orderly positioned on the nanotubular surfaces. As a result, the ZJU-22-based catalytic system showed excellent reactivity for the cross-dehydrogenative coupling (CDC) reaction (Fig. 24d). Wu and coworkers used Mn^{III}Cl-OCPP to connect with paddlewheel $Zn_2(COO)_4$ units for the construction of a porous porphyrinic framework (CZJ-4 CZJ = Chemistry Department of Zhejiang University) with high efficiency and stability upon epoxidation of olefins with excellent substrate size selectivity (Fig. 24e).[125] CZJ-4 was synthesized by the thermal reaction in DMF/acetic acid at 80 ℃ for a week.

CrystEngComm Accepted Manuscript

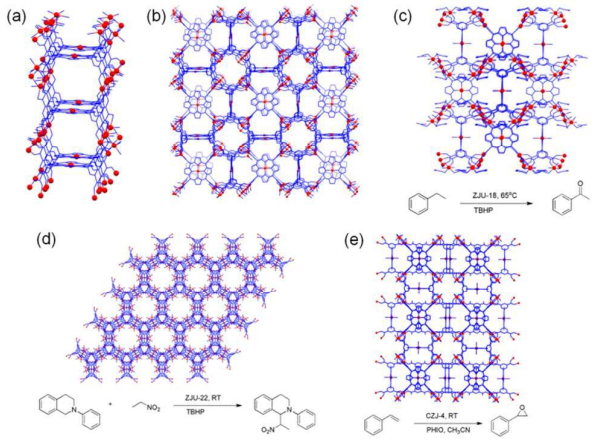

Fig. 24 (a) Structure of MMPF-2 constructed from an octatopic porphyrin H_2TDCPP ligand linking a distorted Co^{II} trigonal prism SBU. Three cobalt porphyrins located in the ''face-to-face'' configuration in MMPF-2. (b) Structure of MMPF-4 containing Zn–TDCPP ligands fused to the square faces of small cubicuboctahedra to afford an augmented **pcu** network with two types of cavities. (c) Structure of ZJU-18 containing a Mn^{III}Cl-H_8OCPP metalloligand connected to binuclear $Mn_2(COO)_4$ and trinuclear $Mn_3(COO)_4(\mu\text{-}H_2O)_2$ SBUs, and the selective oxidation of ethylbenzene catalyzed by ZJU-18 for the formation of phenyl ketone. (d) 3D framework structure of ZJU-22 with 1D nanotubular channels viewed along the *c*-axis, and the cross-dehydrogenative coupling (CDC) reaction of a 1,2,3,4-tetrahydroisoquinoline derivative with nitroalkane. (e) Structure of CZJ-4 viewed along the *c*-axis, and the selective epoxidation of olefins catalyzed by CZJ-4.

Self-assembly of the custom-designed octatopic porphyrin ligand of TDCBPP with Cu_2(carboxylate)$_4$ paddlewheel units under thermal conditions afforded an MMPF-9 with high density of Cu^{II} sites within nanoscopic channels and heterogeneous Lewis-acid catalytic activity for the chemical fixation of CO_2 to form carbonates at room temperature under 1 atm pressure (Fig. 25a).[123]

Zhang and coworkers reported a porph-MOF (UNLPF-1 = University of Nebraska-Lincoln Porous Framework) with eclipsed porphyrin arrays using a single octacarboxylate porphyrin ligand, TBCPPP.[110] The UNLPF-1, $\{[Zn_2(H_2O)_2]_2\cdot[(ZnTBCPPP)(H_2O)_2]\}$, was synthesized by the solvothermal reaction in DMF/acetic acid at 80 ℃ for 72 h. UNLPF-1 is based on a (3,4,4)-connected network with a rare **fjh** topology. Despite a very low uptake of N_2 gas, UNLPF-1 exhibits a high CO_2 capacity and impressive selectivity for CO_2 over N_2. They also constructed an anionic In^{III} porph-MOF (UNLPF-10) by the solvothermal reaction of H_{10}TBCPPP and $In(NO_3)_3H_2O$ in DMF, and UNLPF-10 consists of rare Williams β-tetrakaidecahedral cages (consisting of 14 faces, 24 vertices, and 36 edges) using an octatopic ligand linked with 4-connected $[In(COO)_4]^-$ SBUs (Fig. 25b).[127] The extent of In^{III} metallation of porphyrin macrocycles in UNLPF-10 can control the framework charge density, and UNLPF-10 exhibited excellent photocatalytic activity toward the selective oxygenation of sulfides.

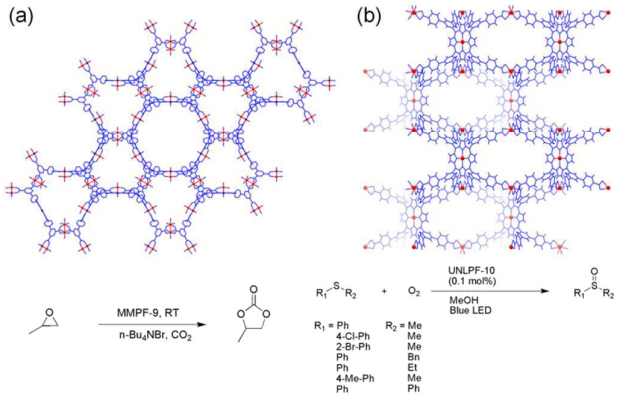

Fig. 25 (a) Structure of MMPF-9 containing truncated triangular channels and hexagonal channels viewed along the *c*-direction, and epoxides coupled with CO_2 catalyzed by MMPF-9 at room temperature under 1 atm pressure. (b) Structure of UNLPF-10 containing octatopic tbcppp ligands and $[In(COO)_4]$ SBUs with the Williams β-tetrakaidecahedral cage, and the photo-oxygenation reactions of sulfides.

Bis(3,5-dicarboxyphenyl)porphyrin and derivatives: H_6BDCPP (5,15-bis(3,5-dicarboxyphenyl)porphyrin, also called H_6DDCPP) and H_6BDCBPP (5,15-bis(dicarboxybiphenyl)porphyrin)

A nanoscopic polyhedral cage-containing MMPF-1 was constructed from the custom-designed porphyrin ligand, BDCPP linking paddlewheel Cu_2(carboxylate)$_4$ SBUs (Fig. 26a) by the solvothermal reaction in DMA.[94] A high density of 16 open Cu^{II} sites within a nanoscopic polyhedral cage of MMPF-1 and the packing of the porphyrin cages via an "ABAB" pattern provide ultramicropores showing selective adsorption of H_2 and O_2 over N_2 and of CO_2 over CH_4.

MMPF-3-generated polyhedral cage-based nanoreactors exhibiting a high density of approximately five catalytically active Co^{II} centers per nm^3 with a custom-designed Co^{II} metalloporphyrin ligand (Fig. 26b).[98] Solvothermally synthesized MMPF-3 exhibits permanent microporosity, superior selectivity and overall conversion in the catalytic epoxidation of *trans*-stilbene compared to the parent **fcu**-MOF-1.

Matsunaga, Mori, and coworkers reported a series of porph-MOFs with a composition of $[Cu_2(MBDCPP)]$ [M = Zn^{II}, Ni^{II}, Pd^{II}, $Mn^{III}(NO_3)$, or $Ru^{II}(CO)$] using MBDCPP [M = Zn^{II}, Ni^{II}, Pd^{II}, $Mn^{III}Cl$, or $Ru^{II}(CO)$] building blocks.[105] They also succeeded in expanding the pore window and interior spaces by using a ZnBDCBPP linker by the solvothermal reaction with $Cu(NO_3)_2\cdot3H_2O$ in DMF/H_2O at 60 ℃ for 24 h (Fig. 26c).[120] The 3D structure of $[Cu_2(ZnBDCBPP)]\cdot5DMF\cdot5H_2O$ is very similar to that of the BDCPP-based MOF[94] and may also be regarded as an assembly of cage structures that consist of eight ZnBDCBPP building blocks and eight Cu_2 paddlewheel SBUs.

CrystEngComm Accepted Manuscript

This journal is © The Royal Society of Chemistry 20xx

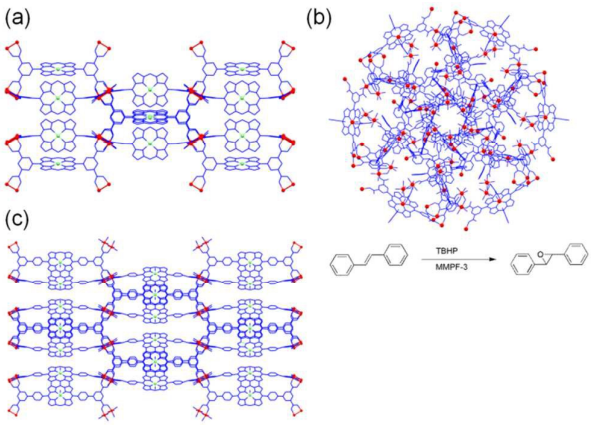

Fig. 26 (a) Structure of $[Cu_2(ZnDDCPP)]$ with cages consisting of eight ZnDDCPP ligands and eight paddlewheel Cu_2 nodes. (b) Structure of MMPF-3 and the *trans*-stilbene epoxidation catalyzed by a heterogeneous MMPF-3 catalyst. (c) Structure of $[Cu_2(ZnBDCBPP)]$ viewed along the crystallographic *b*-axis with a cage consisting of eight ZnBDCBPP ligands and eight paddlewheel Cu_2 nodes.

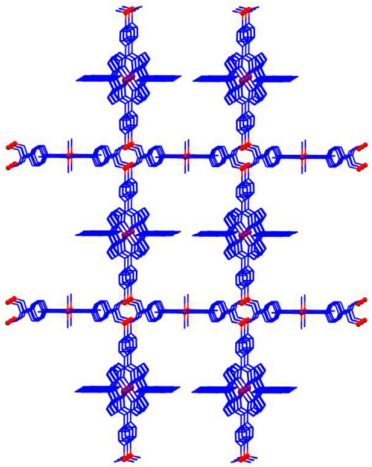

Fig. 27 Structure of the RPM material.

Both H_6TCPP and H_2DPyDF_5PP (5,15-dipyridyl-10,20-bis(pentafluorophenyl)porphyrin)

Hupp and coworkers succeeded in synthesizing a noninterpenetrated, pillared-paddlewheel MOF using TCCP and $DPyF_5PP$ with a Zn salt (ZnPO-MOF) showing a high degree of porosity and containing fully reactant-accessible metalloporphyrin sites.[91] They synthesized porph-MOFs containing a variety of metalloporphyrins (Al^{III}, Zn^{II}, Pd^{II}, Fe^{III}, and Mn^{III} complexes) as components of well-defined, crystalline, highly porous, and stable materials (Fig. 27). These robust porphyrinic materials (RPMs) have large channels with readily accessible active sites. These RPMs are effective catalysts for the oxidation of alkenes and alkanes and are highly stable under oxidative conditions compared to homogeneous catalyst analogues.

Using recently reported RPM materials, Hupp and coworkers examined the systematic exchange of pillaring linkers/struts using a solvent-assisted linker exchange (SALE) technique as a means of accessing new versions of these materials. Dipyridyl-porphyrin Zn^{II} (Zn-dipy) struts were successfully replaced by M^2-dipy ($M^2 = 2H^+$, Al^{III}, Sn^{IV}), forming crystalline solid solutions of $Zn(Zn_{1-x}M_x)$-RPM in variable ratios.[115]

CrystEngComm Accepted Manuscript

Table 2. Carboxyphenyl-based porph-CPs and porph-MOFs.

Compound	Structure	Ref.
{[Cu(TCPP)]$^-$·K$^+$·2H$_2$O·C$_6$H$_5$NO$_2$} {Zn(TCPP)·Na$^+$·1/2(C$_{10}$H$_8$N$_2$)·C$_9$H$_{10}$O$_2$·(CH$_3$OH)$_x$} 	3D 3D	60
[(TCPP)·3(C$_9$H$_{10}$O$_2$)·(C$_7$H$_5$O$_2$)$^-$·Na$^+$] [(ZnTCPP)$^{2-}$· Zn^{2+}·(C$_2$H$_6$O$_2$)$_x$]	2D 3D, diamondoid	61
[(MnTCPP)·(CH$_3$OH)·(H$_2$O)·1.5(C$_9$H$_{10}$O$_2$)] [(ZnTCPP)·(C$_9$H$_{10}$O$_2$)·Na$^+$·(C$_7$H$_5$O$_2$)$^-$] [(ZnTCPP)$^-$·Na$^+$·(CH$_3$OH)·0.5(C$_{14}$H$_8$N$_2$)·3(C$_9$H$_{10}$O$_2$)] [(ZnTCPP)$^{2-}$·(C$_{22}$H$_{20}$N$_4$)$^{2+}$·(C$_{24}$H$_{32}$O$_8$)·4(H$_2$O)]	2D 2D 2D 3D	62
2[TCPP$^-$·Na$^+$]·6C$_6$H$_5$NO$_2$ TCPP$^-$·Na$^+$·4C$_6$H$_5$NO$_2$ 2[ZnTCPP$^-$·Na$^+$·H$_2$O]·4C$_8$H$_{10}$ [2(ZnTCPP)·4Na$^+$·2C$_5$H$_5$N·2OH$^-$]·(C$_{24}$H$_{32}$O$_8$)Na$^+$·12CH$_4$O	2D 2D 2D 2D	63
[CoT(*p*-CO$_2$)PPCo$_{1.5}$(C$_5$H$_5$N)$_3$(H$_2$O)]·11C$_5$H$_5$N (**PIZA-1**)	3D	64
(PdTCPP)$^{4-}$·4K$^+$·6H$_2$O·(CH$_3$)$_2$NCHO (PtTCPP)$^{4-}$·4K$^+$·6H$_2$O·C$_6$H$_5$N (PdTCPP)$^{4-}$·[Cu^{2+}·1½Na$^+$]·½[Cu$^+$(C$_6$H$_5$N)$_3$]·2C$_6$H$_5$N·H$_2$O (PtTCPP)$^{4-}$·[Cu^{2+}·1½Na$^+$]·½[Cu$^+$(C$_6$H$_5$N)$_3$]·2C$_6$H$_5$N·H$_2$O (PtTCPP)$^{4-}$·2[Cu(NH$_3$)$_6$ $^{2+}$]·4H$_2$O	2D	65
[Zn(*p*-CO$_2$)P$_2$-Mes$_2$P]$_3$Zn$_4$O·8H$_2$O (**PIZA-4**) [(*p*-CO$_2$)P$_2$Mes$_2$P = 5,15-di(*p*-carboxyphenyl)-10,20-di(2,4,6-trimethylphenyl)porphyrinate(-2)]	3D	66
Zn(TCPP)(py)·2Zn(H$_2$O)$_2$·1.5(C$_5$H$_5$N)·2(H$_2$O)$_2$ Pt(TCPP)·2Zn(H$_2$O)$_2$·0.5(C$_5$H$_5$N) Pd(TCPP)·2Zn(H$_2$O)$_2$·0.5(C$_5$H$_5$N)	3D	67
[Mn(TCPP)·2(H$_2$O)]·C$_2$H$_6$SO·C$_6$H$_5$NO$_2$ [Mn(TCPP)]·2.55(H$_2$O)·C$_3$H$_7$NO	H-bonded 2D 2D	68
Zn(TPyP)·C$_6$H$_{12}$N$_4$ ·H$_2$O·½(C$_6$H$_5$NO$_2$) Zn(TOHPP)· 2(C$_6$H$_{12}$N$_4$)·2½(C$_6$H$_5$NO$_2$) Zn(TCPP)·2(C$_6$H$_{12}$N$_4$)· 2(C$_9$H$_{10}$O$_2$)	H-bonded 2D	69
(Mn(TpCPP)Mn$_{1.5}$)(C$_3$H$_7$NO)·5C$_3$H$_7$NO (**PIZA-3**)	3D	70
C$_{96}$H$_{82}$N$_8$Ni$_5$O$_{32}$ (Ni$_3$ cluster-TCPP)	3D	71
free-base H$_2$TCPP Mn^{III}-TCPP and Cu^{II}-TCPP [Mn^{III}(Cl)-TOHPP]	H-bonding quadrangular grid networks 2-D	72
Pr$_2$(oxalate)$_3$-H$_2$TCPP Nd$_2$(oxalate)$_3$-H$_2$TCPP Dy$_2$(oxalate)$_3$-H$_2$TCPP	3D 3D 3D	73
CPs by reacting TCPP with common salts of lanthanide metal ions.	3D	74
Porphyrinic MOFs by reacting T*m*CPP with common salts of lanthanide metal ions.	3D	75
{Co[Zn(*cis*-DCPP)(bpy)]}·4DMF·H$_2$O (**PPF-6**) (bpy = 4,4'-bipyridine)	2D, unique CdI$_2$ layers, **kgd**	76
[(Ce^{3+})$_3$(TCPP^{4-})$_2$(HCOO$^-$)(H$_2$O)$_3$] [(Tm^{3+})(C$_{48}$H$_{26.5}$Ca$_{0.25}$N$_4$O$_8$)$^{3-}$(H$_2$O)$_2$]	3D 2D	77
Zn$_2$(ZnTCPP)·3H$_2$O·2DEF (**PPF-1-Zn/Zn**) Co$_2$(CoTCPP)·2H$_2$O·4.75DEF (**PPF-1-Co/Co**)	2D, **sql**, square grid 2D, **sql**, square grid	78
[Co$_2$(CoTCPP)(bpy)$_2$](NO$_3$) (**PPF-3-Co/Co**) [Zn$_2$(ZnTCPP)(bpy)$_{1.5}$] (**PPF-4**) [Co$_2$(PdTCPP)(bpy)] (**PPF-5-Pd/Co**)	AB, 3D, **pcu-b** ABBA, 3D, **fsx** AA, 3D, **fsc**	79
[Zn$_2$(MnTCPP)(bpy)$_2$](NO$_3$) (**PPF-3-Mn/Zn**) [Co$_2$(MnTCPP)(bpy)$_2$](NO$_3$) (**PPF-3-Mn/Co**) [Zn$_2$(FeTCPP)(bpy)$_2$](NO$_3$) (**PPF-3-Fe/Zn**) [Co$_2$(FeTCPP)(bpy)$_2$](NO$_3$) (**PPF-3-Fe/Co**) [Co$_2$(PdTCPP)(bpy)] (**PPF-5-Pd/Co**) [Co$_2$(PtTCPP)(bpy)] (**PPF-5-Pt/Co**) [Zn$_2$(NiTCPP)(bpy)] (**PPF-5-Ni/Zn**) [Zn$_2$(V=OTCPP)(bpy)] (**PPF-5-V=O/Co**)	AB, 3D, **pcu-b** AB, 3D, **pcu-b** AB, 3D, **pcu-b** AB, 3D, **pcu-b** AA 3D, **fsc** AA 3D, **fsc** AA 3D, **fsc** AA 3D, **fsc**	80
[Zn$_2$(ZnTCPP)(DPNI)] (**PPF-18**) [Zn$_2$(ZnTCPP)(DPNI)] (**PPF-19**) [Zn$_2$(ZnTCPP)(DPNI)$_{1.5}$] (**PPF-20**) [Zn$_2$(ZnTCPP)(DPT)] (**PPF-21**) [Zn$_2$(ZnTCPP)(DPT)$_{1.5}$] (**PPF-22**) (DPNI = *N*,*N'*-di-(4-pyridyl)-1,4,5,8-naphthalenetetracarboxydiimide, DPT = 3,6-di-4-pyridyl-1,2,4,5-tetrazine)	bilayer 3D, **fsc** ABBA, 3D, **fsx** bilayer ABBA, 3D, **fsx**	81
Zn$_2$[Zn(*trans*-DCPP)] (**PPF-25**)	3D, **ant**	82
M[TCPP-Et$_4$] [M = Zn (1), Cu (2), Ni (3), and H$_2$ (7)] and TCPP-Me$_4$·H$_2$O (8) Zn[TCPP-Me$_4$] (4), M[TCPP-Me$_4$] [M = Cu (5) and Co (6)]	3D (1) 2D (4)	83
Zn$_2$(ZnTCPP)(dmbpy)·1.1DMF·1.2H$_2$O (**PPF-11-Zn/Zn**) Co$_2$(CoTCPP)(dmbpy)·2.0 DMF·0.2EtOH (**PPF-11-Co/Co**) Zn$_2$(MnTCPP)(dmbpy)·NO$_3$·0.9H$_2$O·4.0DMF (**PPF-11-Mn/Zn**) Zn$_2$(FeTCPP)(dmbpy)·NO$_3$·2.6DMF·1.2MeOH (**PPF-11-Fe/Zn**) (dmbpy = 2,2' -dimethyl-4,4'-bipyridine)	AA, 3D, **fsc** AA, 3D, **fsc** AA, 3D, **fsc** AA, 3D, **fsc**	84
[Cu(TCMOPP)$^{2-}$·Cu^{2+}(H$_2$O)$_2$·(H$_2$O)$_2$] {Zn$_2$[Zn(TCMOPP)(DMF)](DMF)$_2$}·2(DMF)	2D 2D	85
CoTCPP	2D	86
CoTCPP-py-Cu on a surface (**NAFS-1**)	2D	87
[Cd$_{1.25}$(Pd–H$_{1.5}$TCPP)(H$_2$O)]·2DMF	3D	88
Fe(Ni-TCPP)A•(DMF)x (A = Li, Na, K, Rb, Cs; x ~ 3)	3D, **PtS** type	89
[Zn$_4$-(μ$_3$-OH)$_2$(H$_2$O)$_2$(ZnTCPEP-H)$_2$(DABCO)]·2DMF·10.5H$_2$O	3D	90
M$_1$M$_2$-RPMs (M$_1$ designates the metal in L$_1$ (TCPP) and M$_2$ designates the metal in L$_2$ (DPyF$_5$PP)) (**ZnMn-RPM**, **AlZn-RPM**, **FeZnRPM**)	3D	91
Zn$_2$(ZnTCPP)(bpy)·2.5DEF·2H$_2$O (**PPF-27**) **PPF-18** to **PPF-27**, **PPF-20** to **PPF-4** by introduction of the bridging linker BPY	bilayer	92
Zn$_2$(Zn-TCPP)(bodipy) (**BOP**) (bodipy = boron dipyrromethene)	3D	93
Cu$_2$(BDCPP) (**MMPF-1**)	3D, **lvt**-like, nanoscopic cage	94
Fe(Ni-TCPP)A•(DMF)x (A = Li, Na, K, Rb, Cs, x~3)	3D, **PtS**	95
CuTCPP on a gold or silicon surface (**NASF-2**)	2D	96
H$_2$TCPP[AlOH]$_2$(DMF$_3$(H$_2$O)$_2$) (**Al-PMOF**)	3D	97
[Co$_2$(μ$_2$-H$_2$O)(H$_2$O)$_4$](CoDCDBP)·(H$_2$O)$_6$·(C$_2$H$_5$OH)$_{12}$·(DMF)$_{12}$ (**MMPF-3**)	3D, **fcu**, polyhedral cage	98

CrystEngComm Accepted Manuscript

This journal is © The Royal Society of Chemistry 20xx

$Zr_6(OH)_8$-MTCPP (M=Fe, Mn, Co, Ni, Cu, Zn, H_2) (**PCN-222**)	3D, Kagome-type pattern in the ab plane pillared by TCPP	99
{[$Co^{II}_3(OH)(H_2O)]_4(Co^{II}$TDCPP$)_3$}·$(H_2O)_{20}$·$(CH_3OH)_{22}$· $(DMA)_{25}$ (**MMPF-2**)	3D, **msq**	100
[$Pb_2(H_2$TCPP)]·4DMF·H_2O Pb_2(Co–TCPP)(H_2O)(DMF)]·1.5DMF [Pb_2(Ni–TCPP)(DMF)(H_2O)]·1.5DMF·$2H_2O$ [Pb_2(Cu–TCPP)(DMF)(H_2O)]·1.5DMF·$2H_2O$ [Pb_2(VO–TCPP)$(H_2O)_2$]·4DMF	3D 3D 3D 3D 3D	101
PPF-1 to **PPF-27** to **PPF-4** by insertion of BPY **PPF-1** to **PPF-21** by insertion of DPT **PPF-1** to **PPF-18** by insertion of DPNI	bilayer	102
[Zn_{19}(TDCPP$)_3$][$(NO_3)_8$]·$(DMSO)_{61}$·$(H_2O)_{25}$ (**MMPF-4**) [Cd_{11}(TDCPP$)_3$][$(H_3O)_8$]·$(DMSO)_{36}$·$(H_2O)_{11}$ (**MMPF-5**)	3D, **pcu** 3D, **pcu**	103
(Et_2NH_2)[Cd(H_2O)][(H_2TCPP)]·4DEF·H_2O (1) (Et_2NH_2)[Cd(H_2O)][(FeTCPP)]·4DEF·H_2O (1-Fe)	2D	104
[Cu_2(MDDCPP)] [M = Zn^{2+}, Ni^{2+}, Pd^{2+}, $Mn^{3+}(NO_3)$, Ru^{2+}(CO)] using MDDCPP [M = Zn^{2+}, Ni^{2+}, Pd^{2+}, Mn^{3+}Cl, Ru^{2+}(CO)]	3D	105
$Zr_6O_4(OH)_4$(TCPP-$H_2)_3$ (**MOF-525**) $Zr_6O_4(OH)_4(XF)_3$ (**MOF-535**) $Zr_6O_8(H_2O)_8$(TCPP$H_2)_2$ (**MOF-545**) (cruciform H_4-XF = $C_{42}O_8H_{22}$)	3D, **ftw-a** 3D, **ftw-a** 3D, **csq-a**	106
$Zr_6O_8(CO_2)_8(H_2O)_8$-[FeCl(TCPP)] (**MMPF-6**)	3D	107
[Mn_5Cl_2(MnCl-OCPP)$(DMF)_4(H_2O)_4$]·2DMF·$8CH_3COOH$· $14H_2O$ (**ZJU-18**) [Mn_5Cl_2(Ni-OCPP)$(H_2O)_8$]·7DMF·$6CH_3COOH$·$11H_2O$ (**ZJU-19**) [Cd_5Cl_2(MnCl-OCPP)$(H_2O)_6$]·13DMF·$2CH_3COOH·9H_2O$ (**ZJU-20**)	3D, **tbo** 3D, **tbo** 3D, **tbo**	108
CuTCPP (nanofilm)	2D, nanosheet	109
{[$Zn_2(H_2O)_2]_2$·[(ZnTBCPPP)$(H_2O)_2$]} (**UNLPF-1**)	3D, **fjh**	110
$(In_{1.29}O_{0.57}$TCPP$)(C_2H_8N)_{0.71}(CH_3CN)_{1.33}$ $(C_3H_7NO)_{2.50}$ (**MMPF-7**) [In(In-TCBPP)] $(C_3H_7NO)_{12}$ (**MMPF-8**)	3D, **pts** 3D, **pts**	111
$C_{156}H_{60}Cd_8Co_3N_{12}O_{54}$ (**MMPF-5(Co)**)	3D, postsynthetic metal–Ion exchange	112
[Zn_2(MnOH–TCPP)(DPNI)]·0.5DMF·EtOH·$5.5H_2O$ (**CZJ-1**)	3D, cubic α-Po topology	113
$(T^3CPP)_2^-$·$2(CH_3NH_2CH_3)^+$ $(T^3CPP)^{2-}$·$2(DBU-H)^+$ (Co-$T^3CPP)^{4-}$·$2(CH_3NH_2CH_3)^+$·$2(NH_4)^+$ {[Cd(py)$T^3CPP]^{4-}$·[Cd(py)$_3$Cd(py)$_2(H_2O)]^{4+}\}_2$·4(py)·2(MeOH) {[Zn(py)$T^3CPP]^{4-}$·[Zn(py)$_2$Zn(py)$]^{4+}\}_n$·x(py)·y(MeOH) {[Cd(DMF)$T^3CPP]^{4-}$·[Cd(py)(MeOH)Cd(py)$]^{4+}\}_n$·(0.66DMF$)_n$ {[Cd(DMF)$T^3CPP]^{4-}$·[Cd(DMF)(MeOH)Cd(DMF)$]^{4+}\}_n$·(xDMF$)_n$ {[Cd(DMF)$T^3CPP]^{4-}$·4(CdCl)$^+\}_n$·(xDMF$)_n$. (DBU = 1.8-diazabicyclo[5.4.0]undec-7-ene)	H-bonded zigzag chain H-bonded 2D H-bonded 2D 0D 1D 2D 2D 2D	114
M_1M_2-**RPM**	3D	115
[$(CH_3)_2NH_2$][$Zn_2(HCOO)_2(Mn^{III}$–TCPP)]·5DMF·$2H_2O$ [$(CH_3)_2NH_2$][$Cd_2(HCOO)_2(Mn^{III}$–TCPP)]·5DMF·$3H_2O$ [Zn_2(HCOO)$(Fe^{III}(H_2O)$–TCPP)]·3DMF·H_2O [$Cd_3(H_2O)_6(\mu_2$-O)$(Fe^{III}$–HTCPP$)_2$]·5DMF	3D 3D 3D 3D	116
Zr_8O_6-MTCPP(M) (M = no metal, Fe, Cu, Co) (Zr–PCN-221(no metal), Zr–PCN-221(Fe), Zr–PCN-221(Cu), Zr–PCN-221(Co))	3D, **ftw**	117
$Zr_6(\mu_3$-O$)_4(\mu_3$-OH$)_4(OH)_4(H_2O)_4(H_2$TCPP$)_2$ (**PCN-225**) $Zr_6(\mu_3$-O$)_4(\mu_3$-OH$)_4(OH)_4(H_2O)_4$(ZnTCPP$)_2$ (**PCN-225(Zn)**)	3D, **sqc** 3D, **sqc**	118
$Zr_6(OH)_8$-MTCPP (M = no metal, Co, Ni, Fe) (**PCN-224**, **PCN-224(Co)**, **PCN-224(Ni)**, **PCN-224(Fe)**)	3D, **she**	119
[Cu_2(ZnBDCBPP)]·5DMF·$5H_2O$	3D, **sqc3895**	120
CuTCPP (nanofilm)	2D	121
(**DA-MOF**, **L2-MOF**)		122
Cu_6(CuTDCBPP)$(HCO_2)_4(H_2O)_6$ (**MMPF-9**)	3D, **smy**	123
[Cu_4(Ni-OCPP)$(H_2O)_4$]·10DMF·$11H_2O$ (**ZJU-21**) [$Cu_{16}(Mn^{III}$OCPP$)_3(OH)_{11}(H_2O)_{17}$]·21DMF·$65H_2O$ (**ZJU-22**)	3D, **tbo** 3D, **csq-a**, **xly-a**	124
[$Zn_{16}(H_2O)_8(Mn^{III}$Cl-OCPP$)^4$]·19DMF·$34CH_3COOH·45H_2O$ (**CZJ-4**)	3D	125
[$Fe_3O(OOCCH_3)_6$]-MTCPP (**PCN-600(M)** (M = Mn, Fe, Co, Ni, Cu))	3D, **htp-a**	126
In_3TBCPPP (**UNLPF-10**)	3D	127
PCN-224(Fe)-O_2	3D	128
$Zr_6(\mu_3$-O$)_4(\mu_3$-OH$)_4$(Zn–DPDBP$)_6$ (**Zn–DPDBP–UiO**) $Hf_6(\mu_3$-O$)_4(\mu_3$-OH$)_4$(DBP$)_6$ (**DBP–UiO NMOF**)	3D	129
[$Zr_6O_4OH_4(COO)_{12}$]-H_2TCPP (**PCN-223**) [$Zr_6O_4OH_4(COO)_{12}$]-FeTCPP (**PCN-223(Fe)**)	3D, **shp-a**	130
$Co^{III/II}$TCPPCoPIZA (**CoPIZA/FTO**)	3D	131
$(Zr_6(OH)_4O_4$(TCP-1$)_3$·10DMF·$2H_2O$) (**PCN-228**) $(Zr_6(OH)_4O_4$(TCP-2$)_3$·45DMF·$25H_2O$) (**PCN-229**) $(Zr_6(OH)_4O_4$(TCP-3$)_3$·30DMF·$10H_2O$) (**PCN-230**)	3D, **ftw-a**	132
Free-base **PCN-222/MOF-545**		133
[Fe^{III}TCPP$Fe^{III}Cs^I]_n$·xDMF [Fe^{II}TCPP$(Fe^{II}$bpy$)_2]_n$·xDMF [Fe^{II}TCPP$(Fe^{II}$pz$)_2]_n$·xDMF	3D, **pts** 3D, **pcu-b** 3D, **pcu-b** and **fry**	134
[$Zr_6O_4(OH)_4$]-TCBPP (**CPM-99X**, X = H_2, Zn, Co, Fe)	3D	135

Other Porphyrinic MOFs

Goldberg and coworkers reported open 2D arrays of Zn^{II} 5,10,15,20-tetrakis(4-amidophenyl)porphyrin by self-complementary hydrogen bonding between the $-CONH_2$ recognition sites of adjacent molecules, and 1D CPs of Mn^{III} 5,10,15,20-tetraphenylporphyrin perchlorate and the ditopic 4,4'-bpy ligand (Fig. 28a,c).[136] They also used 5,10,15,20-tetrakis(4-cyanophenyl) and 5,10,15,20-tetrakis(4-nitrophenyl) derivatives (Fig. 28b) of Zn^{II}-porphyrin or Cu^{II}-porphyrin as building blocks, characterized modes of self-

CrystEngComm Accepted Manuscript

assembly of these functionalized moieties, and evaluated the utility of such materials in the controlled design of crystalline microporous solids.[137]

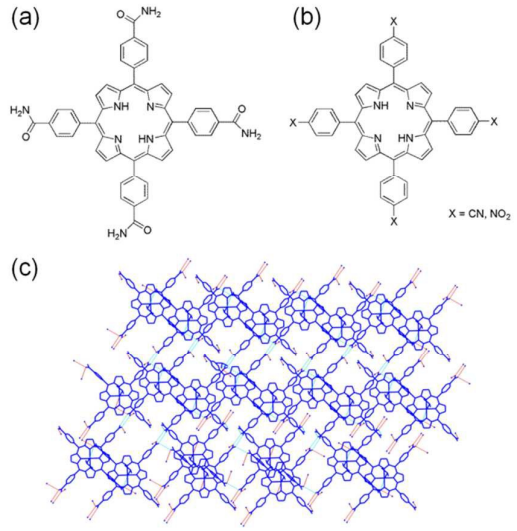

Fig. 28 (a) Chemical structure of 5,10,15,20-tetra(4-amidophenyl)porphyrin. (b) Chemical structure of 5,10,15,20-tetrakis(4-cyanophenyl) and 5,10,15,20-tetrakis(4-nitrophenyl) porphyrins. (c) Assembly of Zn^{II} 5,10,15,20-tetrakis(4-amidophenyl)porphyrin building blocks in the form of 2D open networks sustained by N–H···ONC hydrogen bonds.

Hosseini and coworkers reported 1D and 2D coordination networks assembled from 5,10,15,20-tetrakis(*o*-isonicotinoylamidophenyl)porphyrin (H_2TINAP) and Cu^{II} ions, which are examples of supramolecular isomerism.[138] Either a 1D or 2D coordination network is observed depending on the solvent system (Fig. 29). The free-base H_2TINAP displays four atropisomers because of the bulky isonicotinoyl moieties. They used the $\alpha_2\beta_2$ form among four possible atropisomers (α_4, $\alpha_3\beta$, $\alpha_2\beta_2$, and $\alpha\beta\alpha\beta$).

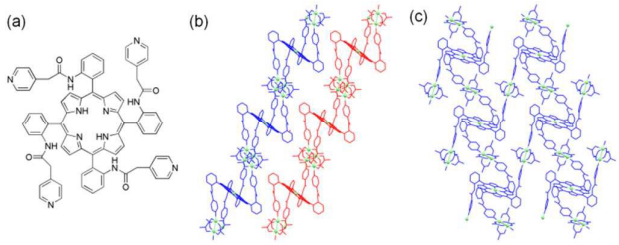

Fig. 29 (a) Chemical structure of 5,10,15,20-tetrakis(*o*-isonicotinoylamidophenyl)porphyrin (H_2TINAP). (b) Crystal structures of the 1D coordination network formed by the self-assembly of the $\alpha_2\beta_2$ form of H_2TINAP and Cu^{II} ions in *i*PrOH/$CHCl_3$, showing the stair-type arrangement and the packing of two consecutive networks. (c) Crystal structures of the 2D coordination network formed by the self-assembly of the $\alpha_2\beta_2$ form and Cu^{II} ions in EtOH/TCE (TCE = 1,1′,2,2′-tetrachloroethane), showing the connection of Cu-metallaporphyrin by $Cu_2(OAc)_4$ SBUs.

Nefedov and coworkers used electron-deficient 5,15-bis(diethoxyphosphoryl)-10,20-diphenylporphyrin (Fig. 30a) to provide an unusually stable 2D Cu^{II} porphyrin network (Fig. 30b).[139] In dioxane, an isolated Cu^{II} porphyrin complex with two axially coordinated dioxane molecules was also prepared. They also reported a supramolecular assembly between the same porphyrin with a Cu_2 paddlewheel-based unit to afford 1D CPs (Fig. 30c).[140]

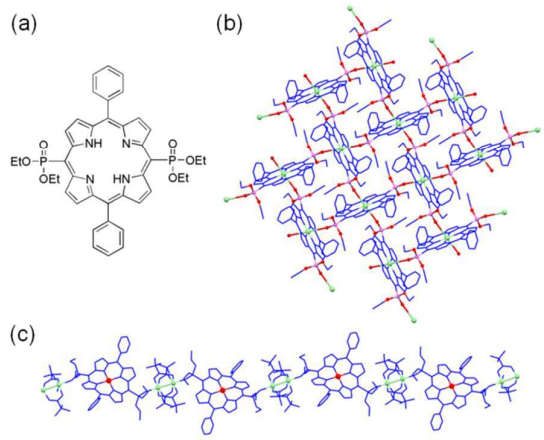

Fig. 30 (a) Chemical structure of 5,15-bis(diethoxyphosphoryl)-10,20-diphenylporphyrin. (b) The unexpected 2D copper CP network. (c) 1D polymer $\{Cu_2(\mu\text{-OOC-t-Bu})_4[\mu\text{-}[O{=}P(OEt)_2]_2(Ph)_2PorNi{\cdot}2CHCl_3]\}_n$.

Guo, Huang, Chen, and coworkers reported a new microporous porph-MOF, $\{Mn^{II}_{0.5}[Mn^{II}_4Cl(Mn^{III}Cl\text{-}TTZPP)_2(H_2O)_4]\}\cdot(DEF)_{20}\cdot(CH_3OH)_{18}\cdot(H_2O)_{12}$ (UTSA-57), that was constructed from (TTZPP = 5,10,15,20-tetrakis[4-(2,3,4,5-tetrazolyl)phenyl]porphyrinato) manganese(III) chloride as the metalloligand (Fig. 31). UTSA-57 was synthesized by the thermal reaction of $MnCl_2{\cdot}4H_2O$ and Mn^{III}Cl-TTZPP in diethylformamide (DEF)/CH_3OH with 6M HCl at 75 ℃ for 48 h, and it adopts the rare **scu** topology with 1D square nanotube-like channels of approximately 20 Å. The activated UTSA-57 exhibits permanent porosity and displays moderately high performance for C_2H_2/CH_4 separation at room temperature.[141]

Zhou and coworkers recently reported PCN-526 prepared from Cd^{II} ions and H_2TTZPP.[142] PCN-526 displays a reversible single-crystal-to-single-crystal phase transition. The modulation of luminescence of PCN-526 was demonstrated by encapsulation of a series of luminescent guest molecules into its pores.

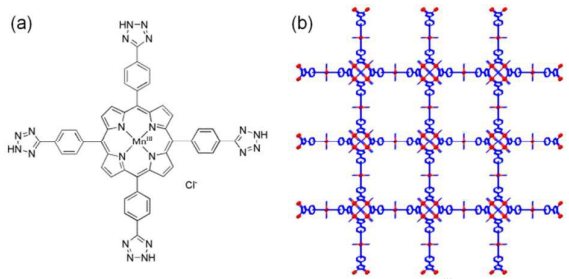

Fig. 31 (a) Chemical structure of the metalloligand Mn^{III}Cl-TTZPP. (b) 3D structure of UTSA-57 with the **scu** topology.

Sun and Liu et al. reported a novel 2D porph-MOF, $[Fe(C_{32}H_{18}N_{12})][Me_2NH_2]$ (NJNU-1, NJNU = Nanjing Normal University) constructed from Fe^{III} ions and 5,10,15,20-tetrakis(4-imidazoyl)porphyrinato (TImP) ligand, which is stable in saturated NaOH solution (Fig. 32).[143] The utilization of an imidazolyl-based porphyrin ligand and a high-valence metal is a new and promising strategy for constructing porph-MOFs with ultra-high stability.

CrystEngComm Accepted Manuscript

This journal is © The Royal Society of Chemistry 20xx

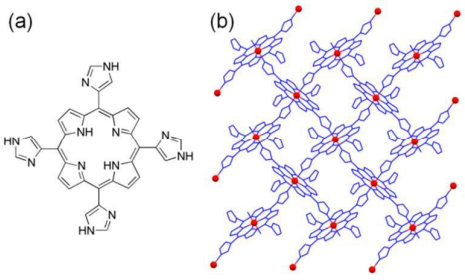

Fig. 32 (a) Chemical structure of H_2TImp. (b) The 2D lamellar network of NJNU-1.

The crystal structures of MgTMPP and ZnTMPP (TMPP = 5,10,15,20-tetrakis(3,4,5-trimethoxyphenyl)porphyrinato) show that they possess an unusual 1D CP structure with metal-oxygen (oxygen atom from the *m*-methoxy group of an adjacent porphyrin) bonds (Fig. 33).[144] MgTMPP displays several distinct nanoscale particle morphologies upon the controlled evaporation of various solvents. Nanospheres, nanorods, and hollow nanospheres can be observed.

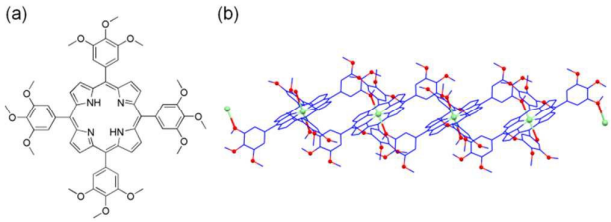

Fig. 33 (a) Chemical structure of H_2TMPP. (b) 1D coordination network of MgTMPP and ZnTMPP.

The sulfonyl-group-containing ligand, 5,10,15,20-tetrakis(4-sulfonatophenyl)porphyrinato (TPPS), leads to the porph-MOF of $[HSm\{V^{IV}O(TPPS)\}]_n$ (Fig. 34) with well-defined 1D channels periodically constricted by porphyrin planes of TPPS bridging ligands.[145] $[HSm\{V^{IV}O(TPPS)\}]_n$ was prepared by the hydrothermal reaction of $SmCl_3{\cdot}6H_2O$, VCl_3 and TPPS in distilled water at 200 ℃ for three days. Interestingly, the N_2-encapsulated crystal structure of the relevant porph-MOF, $[HSm\{V^{IV}O(TPPS)\}]_n \supset N_2$, has also been revealed.

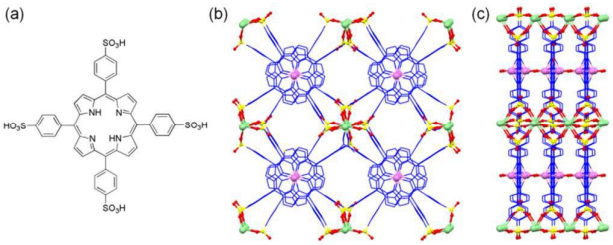

Fig. 34 (a) Chemical structure of H_2TPPS. The framework of $[HSm\{V^{IV}O(TPPS)\}]_n$ along the *c*-aixs (b) and *b*-axis (c).

Conclusions

Various functional porph-MOFs are highlighted based on the types of polytopic porphyrin bridging ligands: (1) porph-MOFs containing 5,10,15,20-tetra(4-pyridyl)porphyrinato (TPyP) bridging ligand and relevant pyridyl-based porphyrin bridging ligands, (2) porph-MOFs formed from 5,10,15,20-tetrakis(4-carboxyphenyl)porphyrinato (TCPP) bridging ligand and relevant carboxyphenyl-based porphyrin bridging ligands, and (3) porph-MOFs containing other miscellaneous custom-designed porphyrin-based bridging ligands. They form various intriguing framework structures as well as porous networks applicable in diverse applications, including CO_2 capture, H_2 and CH_4 storage and separation, energy harvesting, biomedical treatment, and recyclable heterogeneous catalysis. One of the most attractive advantages for developing porph-MOFs is the systematic tunability of both the pore properties and structures of the resulting frameworks by incorporating different chemical functionalities into the porphyrin backbones. Therefore, many new functional porph-MOFs are expected in the future for diverse advanced applications.

Acknowledgments

This work was supported by the Basic Science Research Program of the National Research Foundation of Korea (NRF) funded by the Ministry of Education, Science and Technology (2015R1D1A1A01058136).

Notes and references

‡ Footnotes relating to the main text should appear here. These might include comments relevant to but not central to the matter under discussion, limited experimental and spectral data, and crystallographic data.

1 T. R. Cook, Y.-R. Zheng and P. J. Stang, *Chem. Rev.,* 2013, **113**, 734.
2 M. Eddaoudi, D. F. Sava, J. F. Eubank, K. Adila and V. Guillerm, *Chem. Soc. Rev.,* 2015, **44**, 228.
3 G. Busca, *Chem. Rev.,* 2007, **107**, 5366.
4 J. S. Lindsey, *Chem. Rev.,* 2015, **115**, 6534.
5 M. F. Perutz, M. G. Rossmann, A. F. Cullis, H. Muirhead, G. Will and A. C. T. North, *Nature*, 1960, **185**, 416.
6 M. Gilbert and B. Albinsson, *Chem. Soc. Rev.,* 2015, **44**, 845; A. Tsuda and A. Osuka, *Science*, 2001, **293**, 79; M. C. O'Sullivan, J. K. Sprafke, D. V. Kondratuk, C. Rinfray, T. D. W. Claridge, A. Saywell, M. O. Blunt, J. N. O'Shea, P. H. Beton, M. Malfois and H. L. Anderson, *Nature*, 2011, **469**, 72; P. Parkinson, C. E. I. Knappke, N. Kamonsutthipaijit, K. Sirithip, J. D. Matichak, H. L. Anderson and L. M. Herz, *J. Am. Chem. Soc.,* 2014, **136**, 8217; J. P. Collman, R. Boulatov, C. J. Sunderland and L. Fu, *Chem. Rev.,* 2004, **104**, 561.
7 I. Goldberg, *Chem. Eur. J.,* 2000, **6**, 3863.
8 L. D. DeVries, W. Choe, *J. Chem. Crystallogr.,* 2009**, 39**, 229.
9 B. J. Burnett, P. M. Barron, W. Choe, *CrystEngComm*, 2012, **14**, 3839; B. J. Burnett, W. Choe, *Dalton Trans.,* 2012, **41**, 3889.
10 C. Zou, C. -D. Wu, *Dalton Trans.,* 2012, **41**, 3879.
11 W. -Y. Gao, M. Chrzanowski, S. Ma, *Chem. Soc. Rev.,* 2014, **43**, 5841.
12 E. B. Fleischer and A. M. Shachter, *Inorg. Chem.,* 1991, **30**, 3763.
13 B. F. Abrahams, B. F. Hoskins and R. Robson, *J. Am. Chem. Soc*., 1991, **113**, 3606.

CrystEngComm Accepted Manuscript

14 B. F. Abrahams, B. F. Hoskins, D. M. Michail and R. Robson, *Nature*, 1994, **369**, 727.
15 R. Krishna Kumar and I. Goldberg, *Angew. Chem. Int. Ed.,* 1998, **37**, 3027.
16 K. -J. Lin, *Angew. Chem., Int. Ed.,* 1999, **38**, 2730.
17 D. Hagrman, P.J. Hagrman and Jon Zubieta, *Angew. Chem. Int. Ed.,* 1999, **38**, 3165.
18 C. V. K. Sharma, G. A. Broker, J. G. Huddleston, J. W. Baldwin, R. M. Metzger and R. D. Rogers, *J. Am. Chem. Soc.,* 1999, **121**, 1137.
19 L . Pan, B. C. Noll and X. Wang, *Chem. Commun.,* 1999**,** 157.
20 M. Kondo, Y. Kimura, K. Wada, T. Mizutani, Y. Ito and S. Kitagawa, *Chem. Lett.,* 2000, **29**, 818.
21 Y. Diskin-Posner, G. K. Patra and I. Goldberg, *J. Chem. Soc., Dalton Trans.,* 2001, 2775.
22 L. Pan, S. Kelly, X. Huang and J. Li, *Chem. Commun.,* 2002, 2334.
23 D. Sun, F.S. Tham, C. A. Reed and P.D.W. Boyd, *PNAS,* 2002, **99**, 5088.
24 L. Carlucci, G. Ciani, D. M. Proserpio and F. Porta, *Angew. Chem. Int. Ed.,* 2003, **42**, 317.
25 G. Yucesan, V. Golub, C.J. O'Connor and J. Zubieta, *CrystEngComm*, 2004, **6**, 323.
26 L. Carlucci, G. Ciani, D. M. Proserpio and F. Porta, *CrystEngComm,* 2005, **7**, 78.
27 E. Dieters, V. Bulach and M. W. Hosseini, *Chem. Commun.,* 2005, 3906.
28 S. George and I. Goldberg, *Acta Crystallogr., Sect. E: Struct. Rep. Online*, 2005, **61**, m1441.
29 D. J. Ring, M. C. Aragoni, N. R. Champness and C. Wilson, *CrystEngComm*, 2005, **7**, 621.
30 S. K. Taylor, G. B. Jameson and P. D. W. Boyd, *Supramol. Chem.,* 2005, **17**, 543.
31 T. Ohmura, A. Usuki, K. Fukumori, T. Ohta, M. Ito and K. Tatsumi, *Inorg. Chem.,* 2006**, 45**, 7988.
32 N. Zheng, J. Zhang, X. Bu and P. Feng, *Cryst. Growth Des.,* 2007, **7**, 2576.
33 A. K. Bar, R. Chakrabarty, G. Mostafa and P. S. Mukherjee, *Angew. Chem. Int. Ed.,* 2008, **47**, 8455.
34 S. Lipstman, S. Muniappan and I. Goldberg, *Cryst. Growth Des.,* 2008, **8**, 1682.
35 E. Kuhn, V. Bulach and M.W. Hosseini, *Chem. Commun.,* 2008, 5104.
36 A. M. Shultz, O. K. Farha, J. T. Hupp and S. T. Nguyen, *J. Am. Chem. Soc.,* 2009, **131**, 4204.
37 S. Lipstman and I. Goldberg, *Beilstein J. Org. Chem.,* 2009**, 5***, 77.*
38 R. W. Seidel and I. M. Oppel, *Struct. Chem.,* 2009, **20**, 121.
39 S. Lipstman and I. Goldberg, *Cryst. Growth Des.,* 2010, **10**, 1823.
40 S. Lipstman and I. Goldberg, *CrystEngComm*, 2010, **12**, 52.
41 R.W. Seidel and I.M. Oppel, *CrystEngComm*, 2010, **12**, 1051.
42 R. W. Seidel and I. M. Oppel, *Z. Anorg. Allg. Chem.,* 2010, **636**, 446.
43 E. -Y. Choi, L. D. DeVries, R. W. NoVotny, C. Hu and W. Choe, *Cryst. Growth Des.,* 2010, **10**, 171.
44 S. Lipstman and I. Goldberg, *Cryst. Growth Des.,* 2010, **10**, 4596.
45 S. Lipstman and I. Goldberg, *Cryst. Growth Des.,* 2010, **10**, 5001.
46 L. D. DeVries, P. M. Barron, E. P. Hurley, C. Hu and W. Choe, *J. Am. Chem. Soc.,* 2011, **133**, 14848.
47 M. -H. Xie, X. -L. Yang, C. Zou and C. -D. Wu, *Inorg. Chem.,* 2011, **50**, 5318.
48 N. Shi, L. Xie, H. Sun, J. Duan, G. Yin, Z. Xub and W. Huang, *Chem. Commun.,* 2011, **47**, 5055.
49 C. Zou, Z. Zhang, X. Xu, Q. Gong, J. Li and C. -D. Wu, *J. Am. Chem. Soc.,* 2012, **134**, 87.
50 J. Adisoejoso, Y. Li, J. Liu, P. N. Liu and N. Lin, *J. Am. Chem. Soc.,* 2012, **134**, 18526−18529.
51 Q. Zha, C. Ding, X. Rui and Y. Xie, *Cryst. Growth Des.,* 2013, **13**, 4583.
52 H. -J. Son, S. Jin, S. Patwardhan, S. J. Wezenberg, N. C. Jeong, M. So, C. E. Wilmer, A. A. Sarjeant, G. C. Schatz, R. Q. Snurr, O. K. Farha, G. P. Wiederrecht and J. T. Hupp, *J. Am. Chem. Soc.,* 2013, **135**, 862.
53 S. Jin, H. -J. Son, O. K. Farha, G. P. Wiederrecht and J. T. Hupp, *J. Am. Chem. Soc.,* 2013, **135**, 955.
54 M. S. Saeedi, S. Tangestaninejad, M. Moghadam, V. Mirkhani, I. Mohammadpoor-Baltork and A. R. Khosropour, *Polyhedron*, 2013, **49**, 158.
55 R. Makiura and O, Konovalov, *Dalton Trans.,* 2013, **42**, 15931.
56 L. Pan and Z. Ma, *Mol. Cryst. Liq. Cryst.,* 2014, **605**, 216.
57 H. C. Kim, Y. S. Lee, S. Huh, S. J. Lee and Y. Kim, *Dalton Trans.,* 2014, **43**, 5680.
58 S. H. Chae, H. -C. Kim, Y. S. Lee, S. Huh, S. -J. Kim, Y. Kim and S. J. Lee, *Cryst. Growth Des.,* 2015, **15**, 268.
59 I.-H. Choi, S. H. Chae, S. Huh, S. J. Lee, S. -J. Kim and Y. Kim, *Eur. J. Inorg. Chem.,* 2015, 2989.
60 Y. Diskin-Posner, S. Dahal and I. Goldberg, *Angew. Chem. Int. Ed.,* 2000, **39**, 1288.
61 Y. Diskin-Posner, S. Dahal and I. Goldberg, *Chem. Commun.*, 2000, 585.
62 Y. Diskin-Posner, G. K. Patra, I. Goldberg, *Eur. J. Inorg. Chem.,* 2001, 2515.
63 Y. Diskin-Posner and I. Goldberg, *New J. Chem.*, 2001, **25**, 899.
64 M. E. Kosal, J. H. Chou, S. R. Wilson and K. S. Suslick, *Nat. Mater.*, 2002, **1**, 118.
65 M. Shmilovits, Y. Diskin-Posner, M. Vinodu and I. Goldberg, *Cryst. Growth Des.*, 2003, **3**, 855.
66 D. W. Smithenry, S. R. Wilson and K. S. Suslick, *Inorg. Chem.*, 2003, **42**, 7719.
67 M. Shmilovits, M. Vinodu and I. Goldberg, *Cryst. Growth Des.,* 2004**, 4***,* 633.
68 M. Shmilovits, M. Vinodu and I. Goldberg, *New J. Chem.,* 2004, **28***,* 223.
69 M. Vinodu and I. Goldberg, *New J. Chem.,* 2004, **28**, 1250.
70 K. S. Suslick, P. Bhyrappa, J. -H. Chou, M. E. Kosal, S. Nakagaki, D. W. Smithenry and S. R. Wilson, *Acc. Chem. Res.*, 2005, **38**, 283.
71 R. Kempe, *Z. Anorg. Allg. Chem.*, 2005, **631**, 1038.
72 S. George, S. Lipstman, S. Muniappan and I. Goldberg, *CrystEngComm*, 2006, **8**, 417.
73 S. George, S. Lipstman and I. Goldberg, *Cryst. Growth Des.,* 2006**, 6***,* 2651.
74 S. Lipstman, S. Muniappan, S. George and I. Goldberg, *Dalton Trans.*, 2007, 3273.
75 S. Muniappan, A. Lipstman, S. George and I. Goldberg, *Inorg. Chem.*, 2007, **46**, 5544.
76 E. Y. Choi, P. M. Barron, R. W. Novotney, C. H. Hu, Y. U. Kwon and W. Y. Choe, *CrystEngComm,* 2008, **10**, 824.
77 S. Lipstman and I. Goldberg, *J. Mol. Struct.,* 2008**, 890***,* 101.
78 E. Y. Choi, C. A. Wray, C. H. Hu and W. Choe, *CrystEngComm*, 2009, **11**, 553.
79 E. Y. Choi, P. M. Barron, R. W. Novotny, H. T. Son, C. Hu and W. Choe, *Inorg. Chem.*, 2009, **48**, 426.
80 P. M. Barron, H. T. Son, C. H. Hu and W. Choe, Cryst. Growth Des., 2009, **9**, 1960.
81 H. Chung, P. M. Barron, R. W. Novotny, H. T. Son, C. Hu and W. Choe, Cryst. Growth Des., 2009, **9**, 3327.
82 J. M. Verduzco, H. Chung, C. H. Hu and W. Choe, *Inorg. Chem.*, 2009, **48**, 9060.
83 W. Chen, and S. Fukuzumi, *Eur. J. Inorg. Chem.,* 2009, 5494.

CrystEngComm Accepted Manuscript

This journal is © The Royal Society of Chemistry 20xx

84 P. M. Barron, C. A. Wray, C. Hu, Z. Guo and W. Choe, *Inorg. Chem.*, 2010, **49**, 10217.
85 A. Karmakar and I. Goldberg, *CrystEngComm*, 2010, **12**, 4095.
86 R. Makiura and H. Kitagawa, *Eur. J. Inorg. Chem.,* 2010, 3715.
87 R. Makiura, S. Motoyama, Y. Umemura, H. Yamanaka, O. Sakata and H. Kitagawa, *Nat. Mater.*, 2010, **9**, 565.
88 M. H. Xie, X. L. Yang and C. D. Wu, *Chem. Commun.*, 2011, **47**, 5521.
89 A. Fateeva, S. Devautour-Vinot, N. Heymans, T. Devic, J. -M. Greneche, S. Wuttke, S. Miller, A. Lago, C. Serre, G. D. Weireld, G. Maurin, A. Vimont and G. Ferey, *Chem. Mater.*, 2011, **23**, 4641.
90 S. Matsunaga, N. Endo and W. Mori, *Eur. J. Inorg. Chem.*, 2011, 4550.
91 O. K. Farha, A. M. Shultz, A. A. Sarjeant, S. T. Nguyen and J. T. Hupp, *J. Am. Chem. Soc.*, 2011, **133**, 5652.
92 B. J. Burnett, P. M. Barron, C. Hu and W. Choe, *J. Am. Chem. Soc.,* 2011**, 133***,* 9984.
93 C. Y. Lee, O. K. Farha, B. J. Hong, A. A. Sarjeant, S. T. Nguyen and J. T. Hupp, *J. Am. Chem. Soc.*, 2011, **133**, 15858.
94 X. -S. Wang, L. Meng, Q. Cheng, C. Kim, L. Wojtas, M. Chrzanowski, Y. -S. Chen, X. P. Zhang and S. Ma, *J. Am. Chem. Soc.*, 2011, **133**, 16322.
95 A. Fateeva, S. Devautour-Vinot, N. Heymans, T. Devic, J. -M. Greneche, S. Wuttke, S. Miller, A. Lago, C. Serre, G. D. Weireld, G. Maurin, A. Vimont and G. Ferey, *Chem. Mater.,* 2011, **23**, 4641.
96 S. Motoyama, R. Makiura, O. Sakata and H. Kitagawa, *J. Am. Chem. Soc.*, 2011, **133**, 5640.
97 A. Fateeva, P. A. Chater, C. P. Ireland, A. A. Tahir, Y. Z. Khimyak, P. V. Wiper, J. R. Darwent, M. J. Rosseinsky, *Angew. Chem. Int. Ed.*, 2012, **51**, 7440.
98 L. Meng, Q. Cheng, C. Kim, W. -Y. Gao, L. Wojtas, Y. -S. Chen, M. J. Zaworotko, X. P. Zhang and S. Ma, *Angew. Chem. Int. Ed.*, 2012, **51**, 10082.
99 D. Feng, Z. -Y. Gu, J. -R. Li, H. -L. Jiangt, Z. Wei and H. -C. Zhou, *Angew. Chem. Int. Ed.*, 2012, **51**, 10307.
100 X. S. Wang, M. Chrzanowski, C. Kim, W. -Y. Gao, L. Wojtas, Y. -S. Chen, X. P. Zhang and S. Ma, *Chem. Commun.,* 2012, **48**, 7173.
101 C. Zou, M. -H. Xie, G. -Q. Kong and C. -D. Wu, *CrystEngComm*, 2012, **14**, 4850.
102 B. J. Burnetta and W. Choe, *CrystEngComm*, 2012, **14**, 6129.
103 X. -S. Wang, M. Chrzanowski, W. -Y. Gao, L. Wojtas, Y. -S. Chen, M. J. Zaworotko and S. Ma, *Chem. Sci.*, 2012, **3**, 2823.
104 N. C. Smythe, D. P. Butler, C. E. Moore, W. R. McGowan, A. L. Rheingold and L. G. Beauvais, *Dalton Trans*., 2012, **41**, 7855.
105 S. Matsunaga, N. Endo and W. Mori, *Eur. J. Inorg. Chem.,* 2012, 4885.
106 W. Morris, B. Volosskiy, S. Demir, F. Gándara, P. L. McGriger, H. Furukawa, D. Cascio, J. F. Stoddart and O. M. Yaghi, *Inorg. Chem.*, 2012, **51**, 6443.
107 Y. Chen, T. Hoang and S. Ma, *Inorg. Chem.*, 2012, **51**, 12600.
108 X. -L. Yang, M. -H. Xie, C. Zou, Y. He, B. Chen, M. O'keeffe and C. -D. Wu, *J. Am. Chem. Soc.*, 2012, **134**, 10638.
109 G. Xu, T. Yamada, K. Otsubo, S. Sakaida and H. Kitagawa, *J. Am. Chem. Soc.*, 2012, **134**, 16524.
110 J. A. Johnson, Q. Lin, L. C. Wu, N. Obaidi, Z. L. Olson, T. C. Reeson, Y. -S. Chen and J. Zhang, *Chem. Commun.*, 2013, **49**, 2828.
111 W. -Y. Gao, Z. Zhang, L. Cash, L. Wojtas, Y. -S. Chenb and S. Ma, *CrystEngComm*, 2013, **15**, 9320.
112 X. -S. Wang, M. Chrzanowski, L. Wojtas, Y. -S. Chen and S. Ma, *Chem. Eur. J.*, 2013, **19**, 3297.
113 M. -H. Xie, X. -L. Yang, Y. He, J. Ahang, B. Chen and C. -D. Wu, *Chem. Eur. J.*, 2013, **19**, 14316.
114 S. Lipstman and I. Goldberg, *Cryst. Growth Des.*, 2013, **13**, 942.
115 S. Takaishi, E. J. DeMarco, M. J. Pellin, O. K. Farha and J. T. Hupp, *Chem. Sci.*, 2013, **4**, 1509.
116 C. Zou, T. Zhang, M. -H. Xie, L. Yan, G. -Q. Kong, X. -L. Yang, A. Ma and C. -D. Wu, *Inorg. Chem.*, 2013, **52**, 3620.
117 D. Feng, H. -L. Jiang, Y. -P. Chen, Z. -Y. Gu, Z. Wei and H. -C. Zhou, *Inorg. Chem.*, 2013, **52**, 12661.
118 H. L. Jiang, D. Feng, K. Wang, Z. -Y. Gu, Z. Wei, Y. -P. Chen and H. -C. Zhou, *J. Am. Chem. Soc.*, 2013, **135**, 13934.
119 D. Feng, W. -C. Chung, Z. Wei, Z. -Y. Gu, H. L. Jiang, Y. -P. Chen, D. J. Darensbourg and H. -C. Zhou, *J. Am. Chem. Soc.*, 2013, **135**, 17105.
120 S. Matsunaga, S. Kato, N. Endo and W. Mori, *Chem. Lett.*, 2013, **42**, 298.
121 G. Xu, K. Otsubo, T. Yamada, S. Sakaida and H. Kitagawa, *J. Am. Chem. Soc.*, 2013, **135**, 7438.
122 M. C. So, S. Jin, H. -J. Son, G. P. Wiederrecht, O. K. Farha, J. T. Hupp, *J. Am. Chem. Soc.*, 2013, **135**, 15698.
123 W. -Y. Gao, L. Wojtas and S. Ma, *Chem. Commun.*, 2014, **50**, 5316.
124 X. -L. Yang, C. Zou, Y. He, M. Zhao, B. Chen, S. Xiang, M. O'Keeffe and C. -D. Wu, *Chem. Eur. J.*, 2014, **20**, 1447.
125 X. -L. Yang and C -D. Wu, *Inorg. Chem.*, 2014, **53**, 4797.
126 K. Wang, D. Feng, T. -F. Liu, J. Su, S. Yuan, Y. -P. Chen, M. Bosch, X. Zou and H. -C. Zhou, *J. Am. Chem. Soc.*, 2014, **136**, 13983.
127 J. A. Johnson, X. Zhang, T. C. Reeson, Y. -S. Chen and J. Zhang, *J. Am. Chem. Soc.*, 2014, **136**, 15881.
128 J. S. Andeson, A. T. Gallagher, J. A. Mason and T. D. Harris, *J. Am. Chem. Soc.*, 2014, **136**, 16489.
129 K. Lu, C. He and W. Lin, *J. Am. Chem. Soc.*, 2014, **136**, 16712.
130 D. Feng, Z. -Y. Gu, Y. -P. Chen, J. Park, Z. Wei, Y. Sun, M. Bosch, S. Yuan and H. -C. Zhou, *J. Am. Chem. Soc.*, 2014, **136**, 17714.
131 S. R. Ahrenholtz, C. C. Epley and A. J. Morris, *J. Am. Chem. Soc.*, 2014, **136**, 2464.
132 T. -F. Liu, D. Feng, Y. -P. Chen, L. Zou, M. Bosch, S. Yuan, Z. Wei, S. Fordham, K. Wang and H. -C. Zhou, *J. Am. Chem. Soc.*, 2015, **137**, 413.
133 Y. Liu, A. J. Howarth, J. T. Hupp and O. K. Farha, *Angew. Chem. Int. Ed.*, 2015, **54**, 9001.
134 A. Fateeva, J. Clarisse, G. Pilet, J. -M. Grenèche, F. Nouar, B. K. Abeykoon, F. Guegan, C. Goutaudier, D. Luneau, J. E. Warren, M. J. Rosseinsky and T. Devic, *Cryst. Growth Des.*, 2015, **15**, 1819.
135 Q. Lin, X. Bu, A. Kong, C. Mao, X. Zhao, F. Bu and P. Feng, *J. Am. Chem. Soc.*, 2015, **137**, 2235.
136 R. K. Kumar, S. Balasubramanian and I. Goldberg, *Chem. Commun.*, 1998, 1435.
137 R. K. Kumar, S. Balasubramanian and I. Goldberg, *Inorg. Chem.,* 1998, **37***,* 541.
138 B. Zimmer, V. Bulach, M. W. Hosseini, A. D. Cian and N. Kyritsakas, *Eur. J. Inorg. Chem.*, 2002, 3079.
139 A. A. Sinelshchikova, S. E. Nefedov, Y. Y. Enakieva, Y. G. Gorbunova, A. Y. Tsivadze, K. M. Kadish, P. Chen, A. Bessmertnykh-Lemeune, C. Stern and R. Guilard, *Inorg. Chem.*, 2013, **52**, 999.
140 M. A. Uvarova, A. A. Sinelshchikova, M. A. Golubnichaya, S. E. Nefedov, Y. Y. Enakieva, Y. G.

CrystEngComm Accepted Manuscript

Gorbunova, A. Y. Tsivadze, C. Stern, A. Bessmertnykh-Lemeune and R. Guilard, *Cryst. Growth Des.* 2014, **14**, 5976.
141 Z. Guo, D. Yan, H. Wang, D. Tesfagaber, X. Li, Y. Chen, W. Huang and B. Chen, *Inorg. Chem.*, 2015, **54**, 200.
142 D. Liu, T. -F. Liu, Y. -P. Chen, L. Zou, D. Feng, K. Wang, Q. Zhang, S. Yuan, C. Zhong and H. -C. Zhou, *J. Am. Chem. Soc.*, 2015, **137**, 7740.
143 L. Xu, J. Wang, Y. Xu, Z. Zhang, P. Lu, M. Fang, S. Li, P. Sun and H. -K. Liu, *CrystEngComm*, 2014, **16**, 8656.
144 J. Bhuyan and S. Sarkar, *Cryst. Growth Des.*, 2011, **11**, 5410.
145 W. -T. Chen, Y. Yamada, G. -N. Liu, A. Kubota, T. Ichikawa, Y. Kojima, G. -C. Guo and S. Fukuzumi, *Dalton Trans.*, 2011, **40**, 12826.

Seong Huh *received his BS and MS in Chemistry from Yonsei University (Seoul, Republic of Korea) in 1991 and 1993, respectively, and completed his PhD study at Iowa State University (Ames, USA) in 2004 under the guidance of the late Prof. Victor S.-Y. Lin. He did postdoctoral research at University of California (Berkeley, USA) under the supervision of Prof. John Arnold. He is currently a Professor in the Department of Chemistry, Hankuk University of Foreign Studies (Yongin, Republic of Korea). His research focuses on the preparation and application of metal-organic frameworks, mesoporous oxide materials, nanoscale metallic particles, and heterogeneous catalysts.*

Sung-Jin Kim *received her BS and MS in Chemistry from Ewha Womans University (Seoul, Republic of Korea) in 1981 and 1983, respectively. She received her PhD in Chemistry from Iowa State University (Ames, USA) in 1989. She is currently a Professor in the Department of Chemistry and Nano Science, Ewha Womans University (Seoul, Republic of Korea). Prof. Kim is a member of the Korean Chemical Society and American Chemical Society. Her research focuses on the preparation and application of thermoelectric materials and nano materials (nano catalysts, nano-bio drug delivery, semiconductors, etc.).*

Youngmee Kim *received her BS and MS in Chemistry from Yonsei University (Seoul, Republic of Korea) in 1986 and 1988, respectively. She completed her PhD study in Texas A&M University (College Station, USA) in 1993 under the guidance of the late Prof. F. A. Cotton. She is currently a Research Professor in the Department of Chemistry and Nano Science, Ewha Womans University (Seoul, Republic of Korea). Dr. Kim is a member of the Korean Chemical Society. Her research focuses on the preparation and application of metal-organic frameworks, coordination polymers, and X-ray crystallography.*

CrystEngComm Accepted Manuscript

 This journal is © The Royal Society of Chemistry 20xx

Table of contents

Porphyrinic metal-organic frameworks from custom-designed porphyrins

Seong Huh, Sung-Jin Kim and Youngmee Kim*

This paper highlights porphyrinic metal-organic frameworks (porph-MOFs) assembled from metal ions and custom-designed porphyrins: pyridyl-based, carboxyphenyl-based porphyrins and other custom-designed porphyrins.

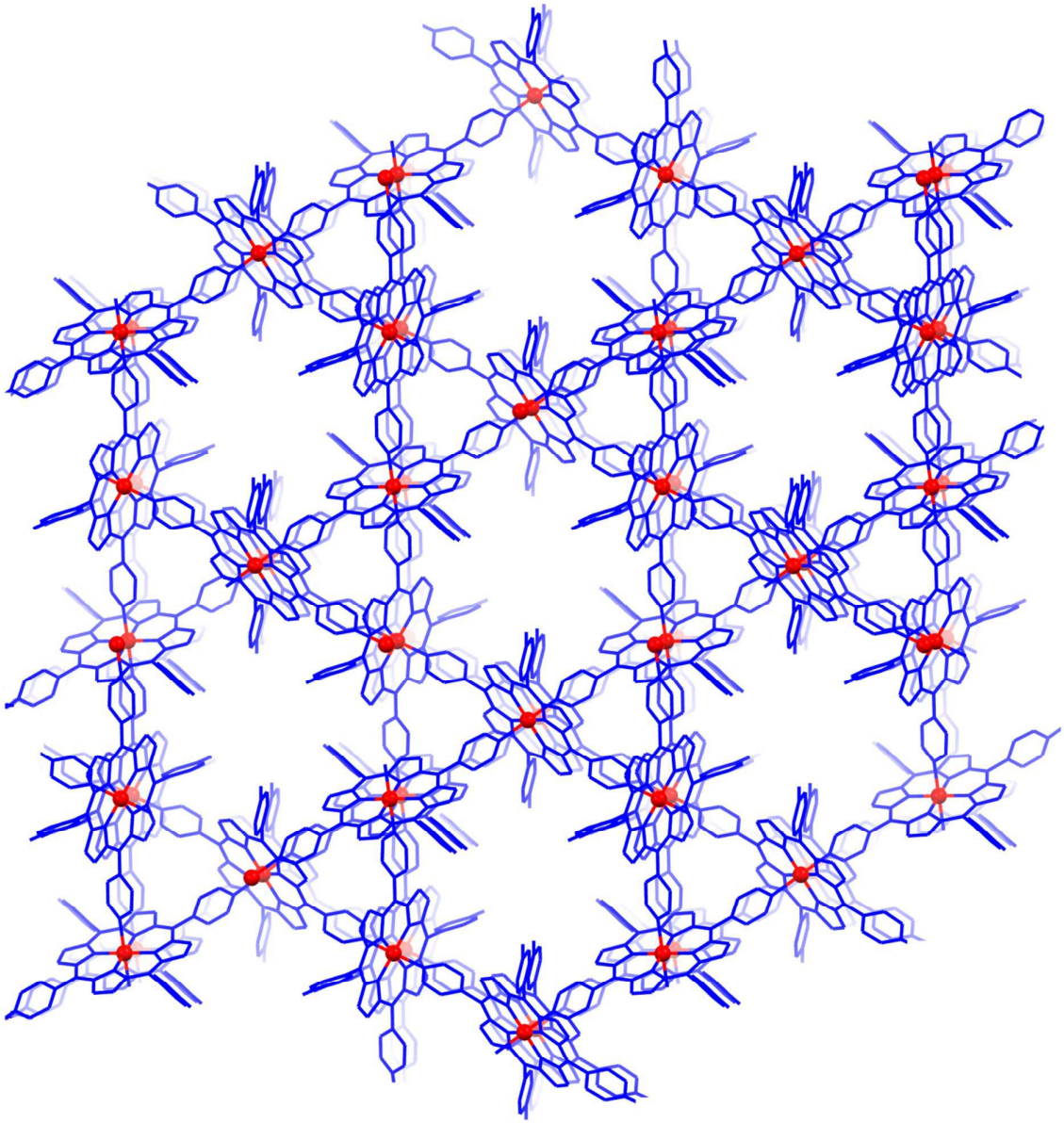

CrystEngComm Accepted Manuscript